ACCURACY COMPARISON OF 2D-3D POINT CORRESPONDENCE FOR POSE ESTIMATION

HANUMANTHA RAO SRINATH

2018

NANYANG TECHNOLOGICAL UNIVERSITY

ACCURACY COMPARISON OF 2D-3D POINT CORRESPONDENCE ALGORITHMS FOR POSE ESTIMATION

HANUMANTHA RAO SRINATH

SCHOOL OF ELECTRICAL AND ELECTRONIC ENGINEERING

2019

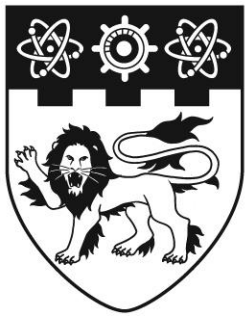

NANYANG TECHNOLOGICAL UNIVERSITY

ACCURACY COMPARISON OF 2D-3D POINT CORRESPONDENCE ALGORITHMS FOR POSE ESTIMATION

HANUMANTHA RAO SRINATH

SCHOOL OF ELECTRICAL AND ELECTRONIC ENGINEERING

2019

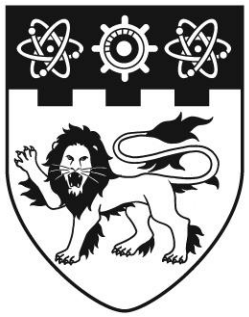

NANYANG TECHNOLOGICAL UNIVERSITY

ACCURACY COMPARISON OF 2D-3D POINT CORRESPONDENCE ALGORITHMS FOR POSE ESTIMATION

HANUMANTHA RAO SRINATH

SCHOOL OF ELECTRICAL AND ELECTRONIC ENGINEERING

A DISSERTATION SUBMITTED IN PARTIAL FULFILMENT OF THE REQUIREMENTS FOR THE DEGREE OF MASTER OF SCIENCE IN COMPUTER CONTROL AND AUTOMATION

2019

Table of Contents:

Abstract

Pose estimation is one of the most basic steps when interfacing a camera with respect to the world. It has seen an increase in usage with the development of autonomy across various fields, mainly robotics. This thesis aims to compare the various 2d-3d point correspondence methods for pose estimation available to us using three different conditions: distance from camera, resolution and pattern used.

There is no documentation available today that describes which pattern, distance and algorithm configuration gives us the best results possible. After getting various correspondences, a hand-eye calibration will be performed and then later used for testing which correspondence environment produces the most accurate results. Accuracy would be the metric used to calculate the results produced from the correspondence algorithms

Acknowledgements

I would like to express my sincere gratitude to Nanyang Technological University for providing me this opportunity to work on this thesis and enhance my academic understanding through the practical application during the course of this thesis.

I am hugely indebted to my project supervisors, Cheah Chien Chern, Associate Professor, School of EEE, Nanyang Technological University and Chen-I-Ming, Professor, School of MAE for allowing me to work on this problem statement through which I was able to update my knowledge in the field of Computer Vision and work with 3-D vision. This proved to be an opportunity for me to further my experience with ROS (Robot Operating System) and OpenCV (Library for Computer Vision) and also improve my skills in coding. I would also like to thank them for their reviews which helped me in completing my project successfully.

List of Figures

Chapter-1: Introduction

1.1 Background:

Pose estimation is one of the vital steps that needs to be performed for automation, especially in the field of robotics. It gives us two basic types of information:

a) Where is the object of interest located with respect to the camera/in the world coordinates?

b) What orientation does the object have?

Using the information above, we can interact with the object accordingly. These two types of information combine to give us DOF (Degrees of Freedom). A pose generally consists of 6 DOF – 3 to describe location (x, y, z) and 3 to describe orientation (roll, pitch, yaw). PnP refers to Perspective-n-Point problem where a set of 3D world points (points in the world) are mapped to the camera pixels so that the camera's position with respect to the object can be known. This is accomplished by using a planar/non-planar object that can be easily identified. In our thesis, only planar objects/patterns will be considered. For PnP to work, the camera in consideration should be calibrated so that the internal calibration parameters (fundamental matrix) is known. Using this information and the planar objects we can estimate the rotation and translation vectors required to transform the object's frame to the camera's frame allowing us to locate the camera in the world frame. This is shown in the picture below.

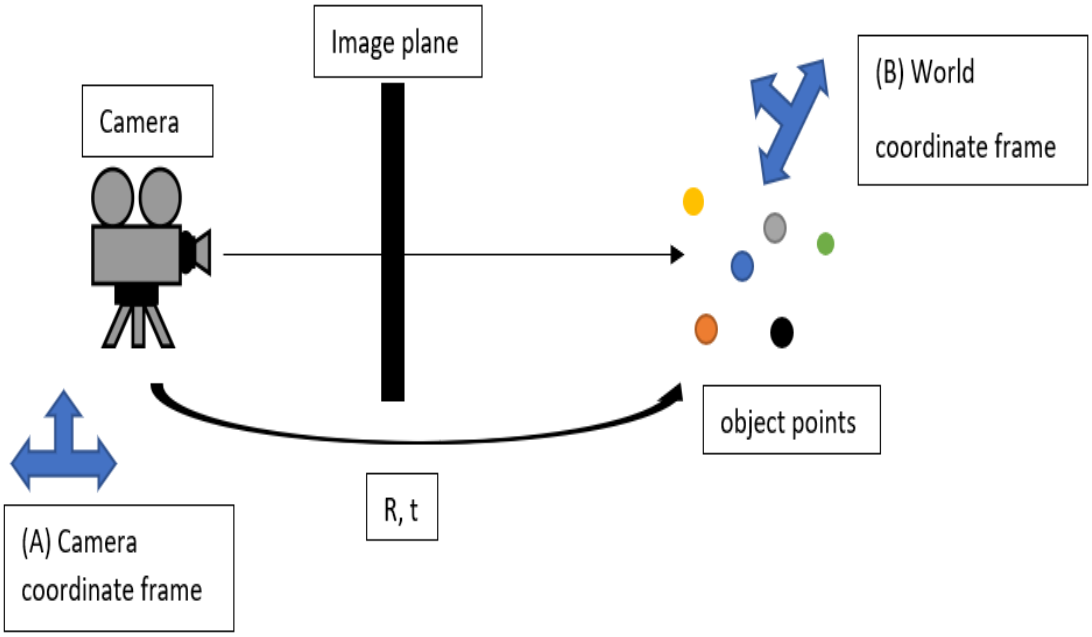

Figure 1: Finding rotation and translation vectors

In the picture above, R and t represent rotation and translation vectors respectively allowing the camera's position to be located with respect to the object. u_o and v_o represent the image points corresponding to the object points.

1.2 Motivation:

Although there have been advances in the algorithms used for PnP problems, there has been no documentation of how each algorithm performs under various conditions. This is important to know as it can help save time and resources when working with real-world

problems. Companies need not waste their resources identifying which pose estimation method suits their needs and can implement the desired algorithm according to the conditions stated. The implementation of these algorithms seems to go unnoticed when used in computer vision libraries such as OpenCV. The solvepnp method present in OpenCV uses the Iterative method as the default one. Users do not know how well the other algorithms perform on the same data they are using or they cannot judge therefore they seem to utilize the default method. The usage of patterns when solving the PnP problem is also a major question as there are various patterns available today: Checkerboards, Aruco markers, Ellipse markers and many more. There is again no documentation about the usage of markers and the corresponding accuracies derived from using them with various algorithms involved.

1.3 Objective and Scope:

The objective of this thesis is to identify the best working algorithms used in PnP solutions under various conditions. The varying conditions are:

a) Change in position (distance from camera to object)

b) Change in resolution

c) Change in markers

As every experiment is devised, we would also require control variables. The illumination, waypoints of the robot, robotic arm used, hand-eye calibration method used is kept constant to ensure these discrepancies don't affect the accuracy of the solutions.

After estimating the camera position for different waypoints, a hand-eye calibration is performed to test the accuracy of the calibration that directly informs us of the accuracy of the PnP algorithm/marker solutions.

1.4 Organization of the Dissertation:

Chapter 1: This chapter introduces and gives the basic information on pose estimation as well as the motivation and objectives to carry out the thesis.

Chapter 2: The literature review discusses the information/papers reviewed, which provided an insight on avoidance of pose estimation, hand-eye calibration, and the various PnP algorithms used.

Chapter 3: The experimental setup along with the hardware and software used are discussed in this section

Chapter 4: This section details the methodology of the experiment

Chapter 5: This section discusses the results and findings of the experiment

Chapter 5: The conclusion/summary and future work is discussed in this section

Chapter-2: Literature Review

The various information required to start working on pose estimation solutions are given below.

2.1 The Pinhole Camera Model and Internal Calibration

The pinhole camera was invented in the 20th century. It produces an inverted image on a film. We will be using the pinhole camera model to calibrate and get the intrinsic parameters of the camera. These parameters later are used to calculate the pose of the object.

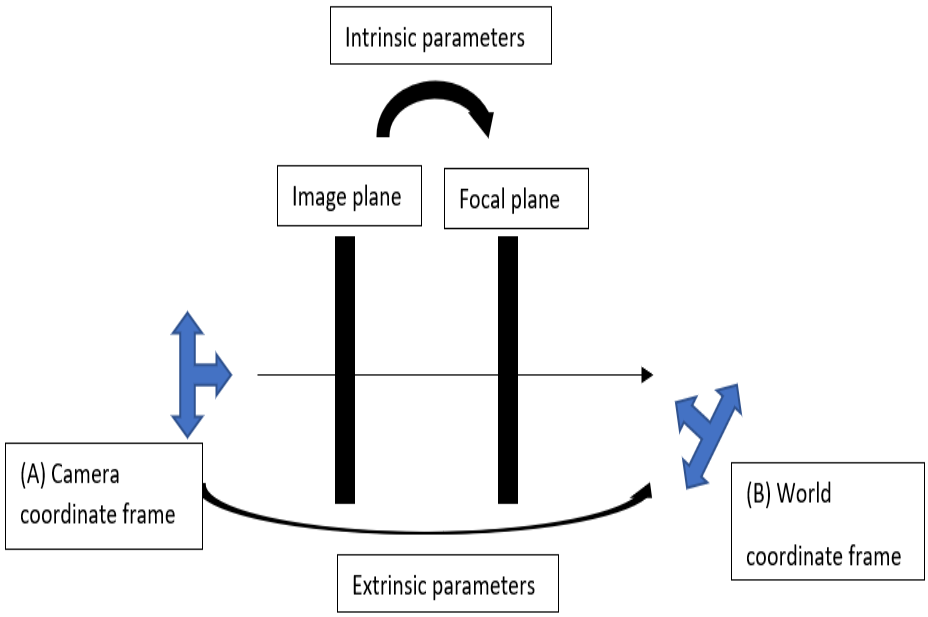

Figure 2: Intrinsic and Extrinsic parameters

As mentioned before, the extrinsic parameters are the rotation and translation vectors that are used to identify the pose of the given object. Internal calibration allows us to identify key special parameters. The intrinsic/internal calibration maps the focal plane(film) onto the camera hole.

$$K = \begin{pmatrix} f_x & s & x_0 \\ 0 & f_y & y_0 \\ 0 & 0 & 0 \end{pmatrix} \quad (1)$$

where:

f_x and f_y represent x and y components of the focal length

x_0 and y_0 represent the x and y components of how much the image center is offset from the center of the image plane

The pinhole camera is characterized by the formula above [1]. The parameters f_x and f_y represent the focal length. The focal length is the distance between the film and the camera's pinhole in pixels. A perfect pinhole camera would not have the x and y components but would have just one focal length. The x_0 and y_o represent the offsets. The principal axis is a line that passes through the pinhole and intersects the film perpendicular to it. The x_0 and y_0 tell us about the offset of the centre of the film from the principal axis. Again, a perfect pinhole camera would not have any offsets. The process of calculating these values is called as internal calibration.

$$\begin{pmatrix} x \\ y \\ w \end{pmatrix} = \begin{bmatrix} f_x & s & c_x \\ 0 & f_y & c_y \\ 0 & 0 & 0 \end{bmatrix} \begin{bmatrix} X \\ Y \\ Z \end{bmatrix} \quad (2)$$

where:

f_x and f_y represent x and y components of the focal length

c_x and c_y represent the x and y components of how much the image center is offset from the center of the image plane

X, *Y* and *Z* – world coordinates

x, *y* and *w* – homogenous image coordinates

The use of w is to ensure that the system is homographic. Along with finding these characteristics it is important that we also reduce the distortion. The radial and tangential distortion is as given below

$$x_{corrected} = x(1 + k_1 r^2 + k_2 r^4 + k_3 r^6) \quad (3)$$

$$y_{corrected} = x(1 + k_1 r^2 + k_2 r^4 + k_3 r^6) \quad (4)$$

where:

k_1, k_2 and k_3 are distortion parameters.

These parameters are calculated by producing a set of simultaneous equations for each frame. A commonly used marker such as a checkerboard is fed as an image and the

interspacing values are provided. Each picture provides a n equation for the above formulae allowing us to calculate the parameters by convergence.

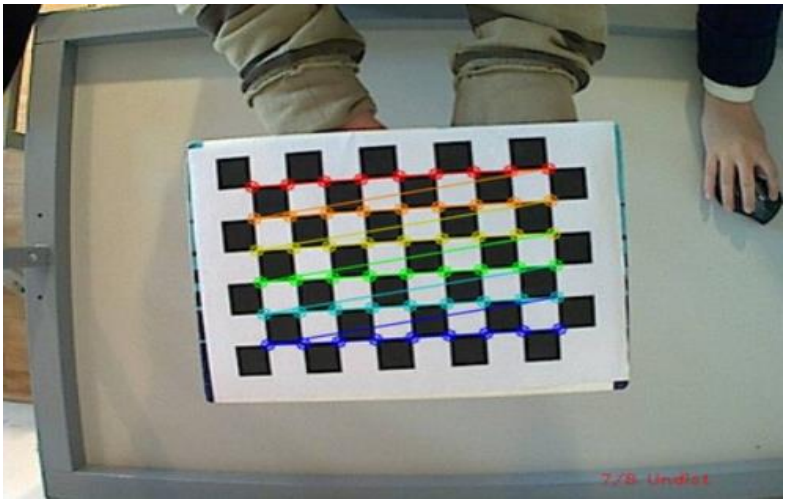

Figure 3: Marker for calculating intrinsic parameters

In the picture above, we can see that the points are identified on the image. These points are then mapped to the real-world coordinates and the parameters are calculated with ease by taking numerous pictures of the checkerboard at various angles to reduce distortion and increase accuracy of calculated values.

2.2 Hand-Eye Calibration

The hand-eye calibration allows us to locate the location of the camera in world coordinates. This helps us to easily identify the objects of interest located in the world corresponding to the ones in the image. Several pose estimation values are mapped along with the robot's location in the world to calculate the location of the camera frame in the world frame

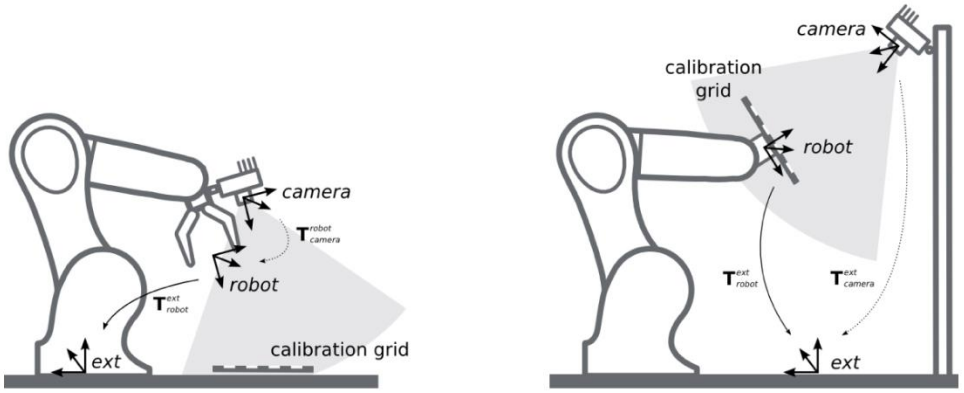

Figure 4: Configurations for calibration

Here, there are two configurations shown. The first configuration has the camera mounted on the robot whereas the second configuration has the grid/pattern mounted on the robot. The objective of the calibration is to identify where the real coordinates of the image points are. The first configuration is called eye-in-hand and the second is called eye-of-hand. We will be utilizing the eye-of-hand configuration in this thesis.

The steps of a hand-eye-calibration are described below

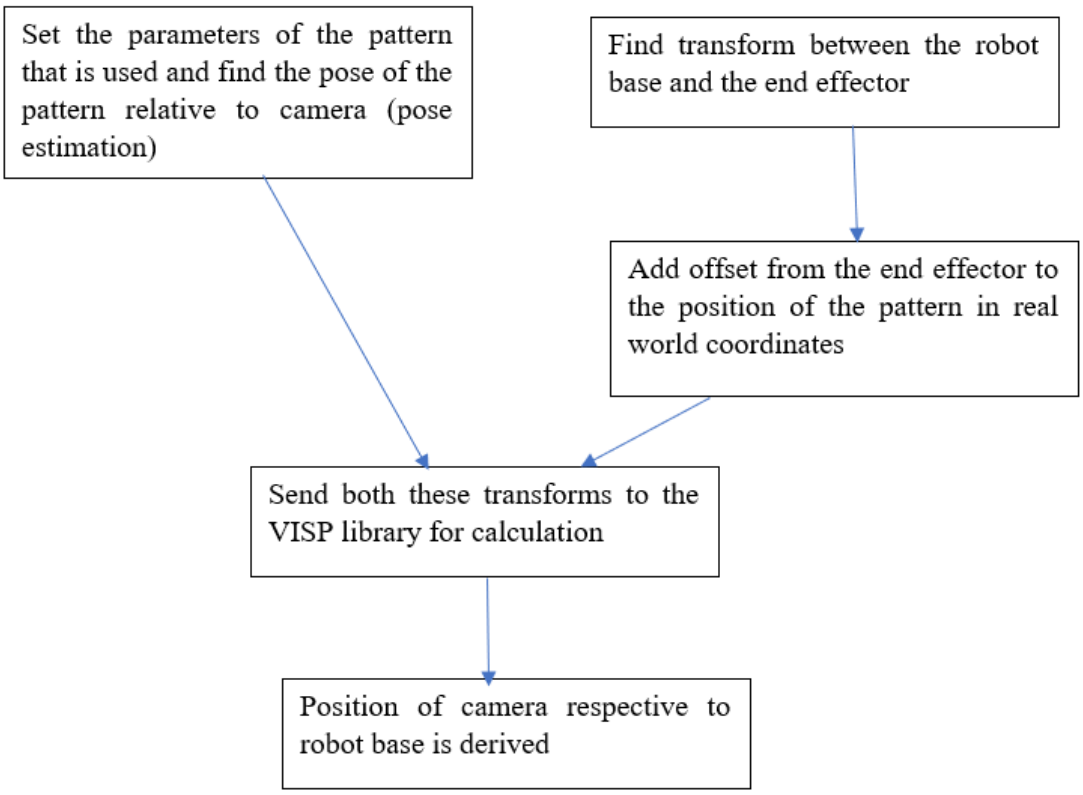

Figure 5: Workflow of hand-eye calibration

The pose estimation is first carried out to get the transformation of frames from the camera to the object/pattern. Later the transform from the robot base to the end effector is calculated, factoring in the offset from the end effector to the pattern being identified in the camera. Both these transformations are sent to the VISP library to output a transformation that gives us the final position of the camera respective to the base of the robot.

Our solution for hand-eye is given as below

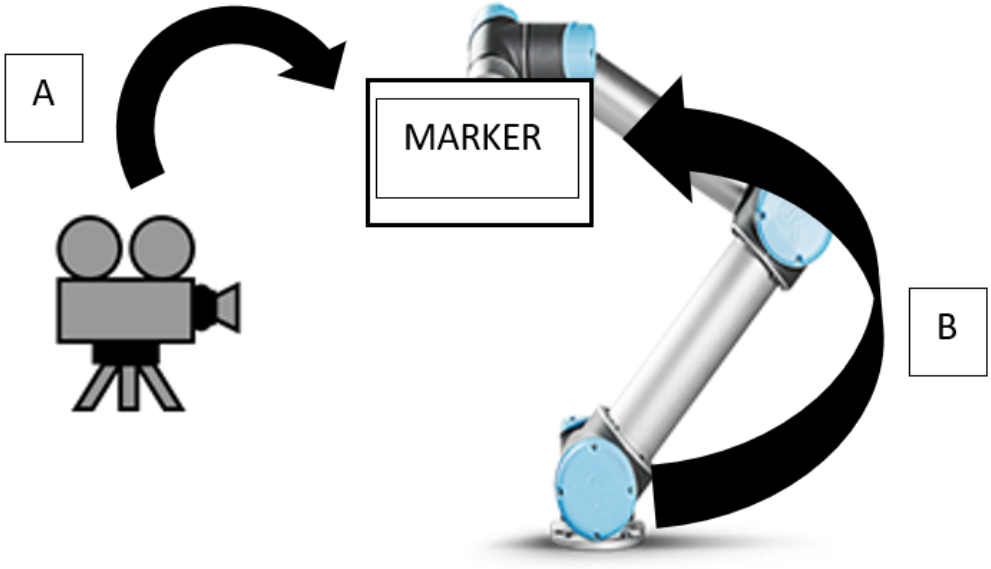

Figure 6: Calibration transformations

where:

A: Transform between camera and pattern

B: Transform between robot base and end offset

X: Transform between camera and robot base.

The transformations are calculated for a series of movements and positions of the pattern and sent to the VISP library [2]. The library computes the transformations and converges to provide us with one value of rotation and translation allowing us to identify where the camera is located in the real world with respect to the robot. The VISP library will not be discussed much in detail as it is out of the scope of this thesis.

2.3 Pose Estimation

To find a pose of the object(planar) we consider the object to be at no height(Z=0). This ensures that we find the position of the camera in space. After finding the pattern, we run the solvepnp function to get the rotation/translation vectors to get the transformation from camera to object/pattern. The process is described in a flowchart before.

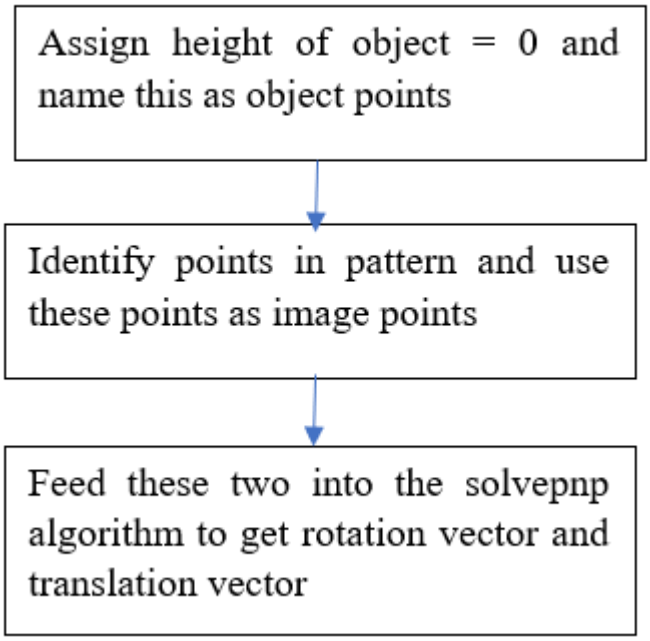

Figure 7: Flowchart to describe pose estimation algorithm structure

The solvepnp [3][4] method utilizes algorithms to produce the rotation and translation vectors. These algorithms will be discussed in further detail in the next section. We will

be utilizing three different algorithms for the experiment. Levenberg-Marquardt Optimization, EPNP and P3P namely.

2.3.1 Levenberg Marquardt Optimization

This method[5][6][7] first utilizes a direct linear transform method and then moves on to use Levenberg Marquardt Optimization to ensure that the dof of R is reduced from 9 to 3.

There is a visual constraint here that the angle between two image points is the same as the angle between two points in the world coordinates. This angle helps us to find the vectors.

$$\begin{pmatrix} X \\ Y \\ Z \end{pmatrix} = R \begin{pmatrix} U \\ V \\ W \end{pmatrix} + t \tag{5}$$

where:

X, Y and *Z* are world coordinates

U, V and *W* represent image coordinates

R represents the rotation vector

t represents the translation vector

The equation described above is the final form to find extrinsic parameters. When expanded, the equation looks like the one below.

$$\begin{pmatrix} X \\ Y \\ Z \end{pmatrix} = \begin{bmatrix} r_{00} & r_{01} & r_{02} & t_x \\ r_{10} & r_{11} & r_{12} & t_y \\ r_{20} & r_{21} & r_{22} & t_z \end{bmatrix} \begin{bmatrix} U \\ V \\ W \end{bmatrix} \quad (6)$$

where:

X, *Y* and *Z* are world coordinates

U, *V* and *W* represent image coordinates

r_{xy} represents the rotation matrix

$t_{x\text{-}z}$ represents the translation vector

If we find out a minimum number of correspondences between the image points and the world points, we can solve for the r and t variables with a series of linear equations.

This is easily solvable but we notice an addition of s into the equation that appears from the intrinsic matrix. This complicates the equation and thus it cannot be solved directly.

$$s\begin{pmatrix} X \\ Y \\ Z \end{pmatrix} = \begin{bmatrix} r_{00} & r_{01} & r_{02} & t_x \\ r_{10} & r_{11} & r_{12} & t_y \\ r_{20} & r_{21} & r_{22} & t_z \end{bmatrix} \begin{bmatrix} U \\ V \\ W \end{bmatrix} \quad (7)$$

where:

X, *Y* and *Z* are world coordinates

U, *V* and *W* represent image coordinates

r_{xy} represents the rotation matrix

$t_{x\text{-}z}$ represents the translation vector

s represents skew

We will thus employ a Direct Linear Transform [8][9][10][11] method here where we solve for the unknowns r and t. We can always use a DLT method when we see a linear equation is off by some scale.

After utilizing the DLT, we notice that our rotation vector has 9 degrees of freedom but we only require 3 (roll, pitch and yaw). One way of finding out the R and t vectors would be to minimize the reprojection error (sum of squared distances between 2d and 3d points). We have to keep modifying R and t to ensure that the reprojection error reduces. This is easily achievable by using the Levenberg-Marquardt optimization technique that uses the Gradient descent method by finding the local minima.

2.3.2 EPnP (Efficient Perspective-n-Point) Algorithm

This method[12][13] utilizes a selection of 4 control points. The points can be chosen arbitrarily or taking the centroid of the reference points as one and the rest are chosen to form a basis that aligns with the principal directions. The equation below describes the control points

$$p_i^w = \sum_{j=1}^{4} \propto_{ij} c_j^w \text{ with } \sum_{j=1}^{4} \propto_{ij} = 1 \quad (8)$$

$$p_i^c = \sum_{j=1}^{4} \propto_{ij} c_j^c \text{ with } \sum_{j=1}^{4} \propto_{ij} = 1 \quad (9)$$

where:

P^w refers to control points in the world coordinates

P^c refers to control points in the camera coordinates.

α refers to barycentric coordinates

Once the coordinates are calculated, we have to utilize a Gaussian Newton iteration to reduce dimensionality and constraints to produce a stable result.

Before embarking on this, since our case is planar, we will be using the N=4 case where we have to derive M – whose kernel the solution must lie in.

The Gaussian Newton optimization error should be minimized to reduce error in β.

After this step, we can get the best β and thus the best P^c and P^w and compute the Rotation and Translation vectors accordingly. We notice that in the planar case, the

dimensionality of M is reduced to 2nx9 having 9D eigenvectors. Although the number of quadratic constraints drop from 6 to 3, we need to linearize again.

2.3.3 Perspective-3-Point (P3P)

The P3P algorithm [14][15][16] only takes 3 correspondences between image and world points. Since it produces a lot of solutions, we use a 4^{th} point to ensure ambiguity is removed in the solution and a stable result is produced.

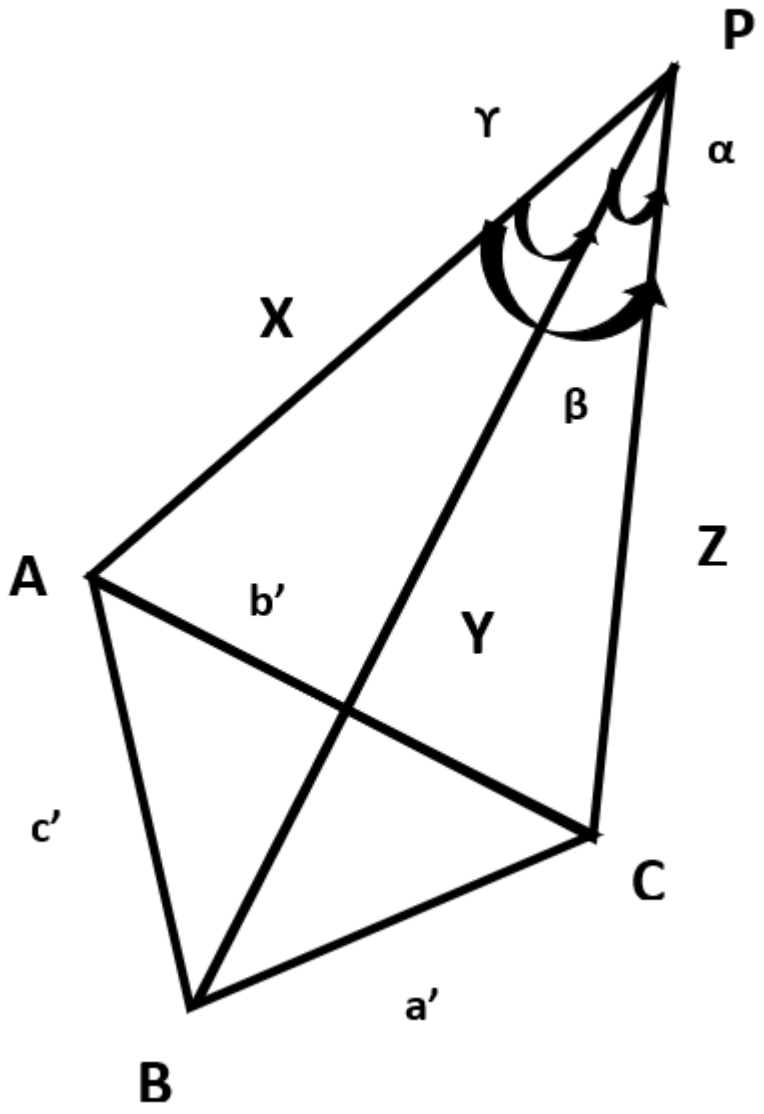

Figure 8: Equations for P3P

where:

X, *Y* and *Z* are world coordinates

$a, b, c, \alpha, \beta, \Upsilon$ are as shown in the image

Replace the variables by the ones given below:

$$X = xZ$$

$$Y = yZ$$

$$c'^2 = vZ^2$$

$$a'^2 = avZ^2$$

$$b'^2 = bvZ^2 \quad (10)$$

We must know that the points P, A, B and C are non-co-planar. Once this is done, we use the law of cosines to get the formula below.

$$Y^2 + Z^2 - 2YZ\ cos \propto = a'^2 \quad (11)$$

$$X^2 + Z^2 - 2YZ\ cos\beta = b'^2 \quad (12)$$

$$X^2 + Y^2 - 2YZ\ cos\gamma = c'^2 \quad (13)$$

The variables are substituted according to (10)

$$y^2Z^2 + Z^2 - yZ^2p = avZ^2 \quad (14)$$

$$x^2Z^2 + Z^2 - xZ^2q = bvZ^2 \quad (15)$$

$$x^2Z^2 + y^2Z^2 - xyZ^2p = vZ^2 \quad (16)$$

Dividing by Z^2 and Replacing v as $x^2 + y^2$

$$(1-a)y^2 - ax^2 + axyr - yp + 1 = 0 \quad (17)$$

$$(1-b)x^2 - by^2 + bxyr - xq + 1 = 0 \quad (18)$$

This algorithm can have many solutions so it is essential that we use a 4th point to determine the best answer.

$$Z = \frac{c'}{\sqrt{v}} \quad (19)$$

Using (19) we can calculate R and t through matrix multiplication.

All the three methods produce outliers. To remove them and to not let these outliers affect the computation of rotation and translation vectors, we utilize a method called solvepnpransac that takes care of these.

Chapter 3: Experimental Setup

This chapter introduces and explains the hardware and software that was used for experimentation along with the entire setup. The specifications of the hardware used are explained and the motivation behind choosing them. The various configurations for the

experimentation are explained in detail in this chapter. A brief explanation about the software used is also provided along with the benefits.

3.1 Hardware used

3.1.1 UR5 (Universal Robot 5) Robot Arm

The Universal Robot Arm 5 was used in experimentation for utilization in hand-eye calibration to ensure the accuracy of the algorithms and patterns used.

Figure 9: UR5 and teach pendant

The UR5 arm has the following specifications

- Payload: 5 kg,
- Weight: 20.6 kg,
- Reach: 850mm

The teach pendant that comes with the UR5 allows us to store certain values as waypoints. These values were later used as the control waypoints when calibrating the robot with the camera.

3.1.2 Zed Camera

The Zed stereovision camera was selected for its ease of use and ROS connectivity.

Figure 10:ZED Camera

The ZED camera has the following features

RESOLUTION	FRAMES PER SECOND
2K	15
1080P	30

720P	60
WVGA	100

Depth range – 0.5-20m

3.2 Software and drivers used

3.2.1 ROS

The system to be calibrated requires a common ground for sending and receiving messages and data so that we don't need to create a separate communication channel and perform all these tasks simultaneously. ROS (Robot Operating System) allows us to perform the functions listed above.

Ros introduces a system of nodes that allows executables(programs) to run simultaneously and be coupled (integrated). It acts as a middleware between the operating system and the devices/robots.

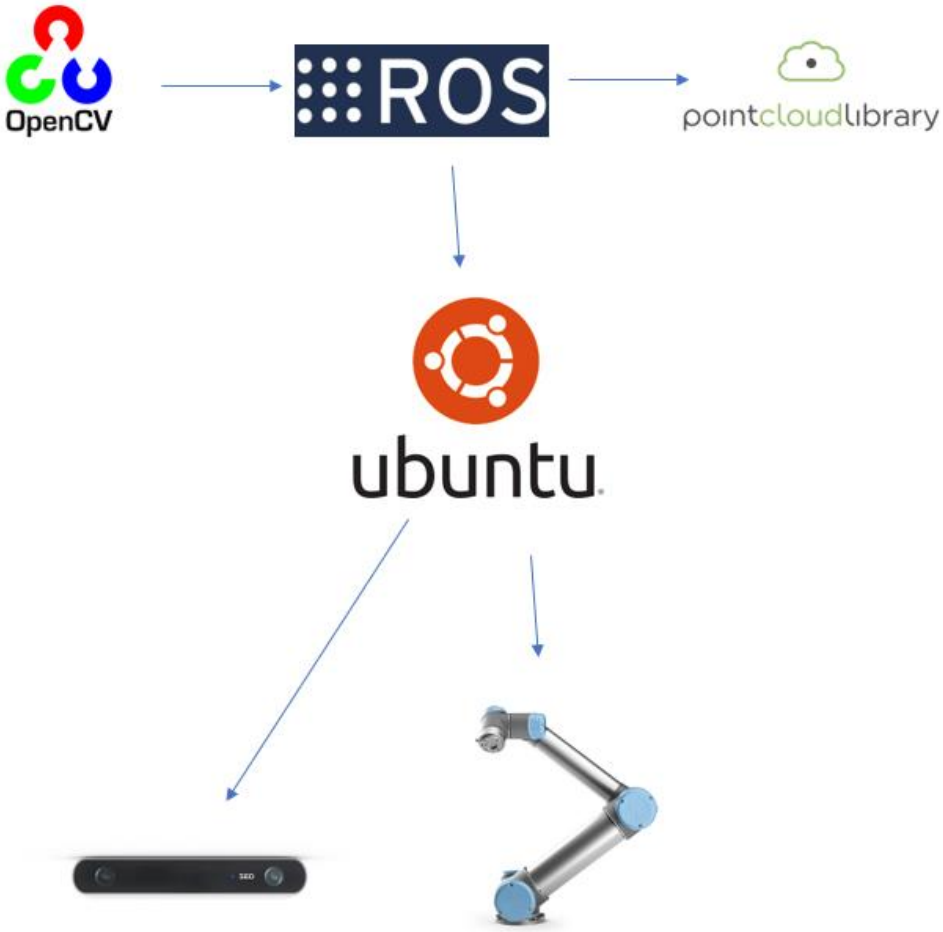

Figure 11: Example ROS flowchart

The picture above demonstrates an example of how a ROS process looks like. The software is able to work with a multitude of libraries making it easy for accessing and implementation while also connecting with a plethora of I/O devices.

3.2.2 OpenCV

OpenCV is a computer vision/image processing library that is used as a common infrastructure for computer vision applications and to accelerate use of machine learning.

OpenCV has a lot of functions built in and reduces the need to code every single mathematical equation that we need.

It can be used with both C++ and Python as well as interfacing with ROS helping systems to integrate with ease.

3.2.3 Pointclouds and PCL (Point cloud library)

Pointclouds are sets of data points that are outputs from 3d vision cameras. They are present in 3d space and have 4 major features (x, y, z and intensity).

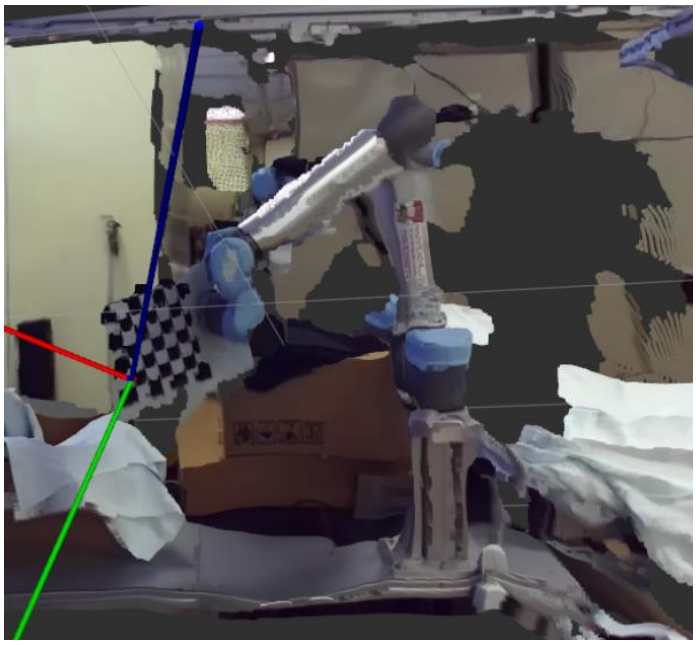

Figure 12: Pointcloud example

The pointcloud library helps us to interact and modify these 3d data points with ease. For our thesis we would require the pointcloud to verify if the algorithms are producing the pose with a good accuracy.

3.2.4 UR Driver

The UR driver can be interfaced with ROS. It helps to publish the robot model information and TF (Transformation trees). The TF trees can help us identify the transformation between the end effector and the base of the robot allowing us to provide it as an input to the hand-eye calibration model directly. An example of the robot model visualization and tf are given below.

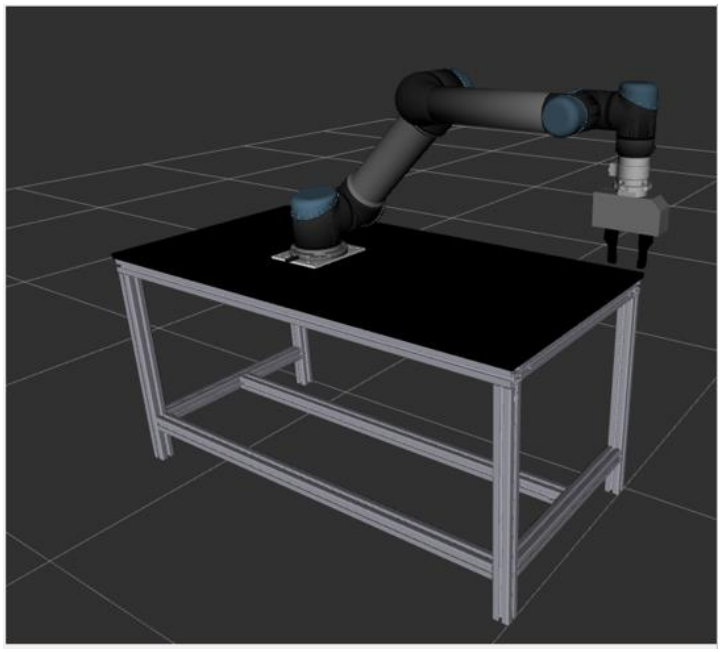

Figure 13:Robotmodel

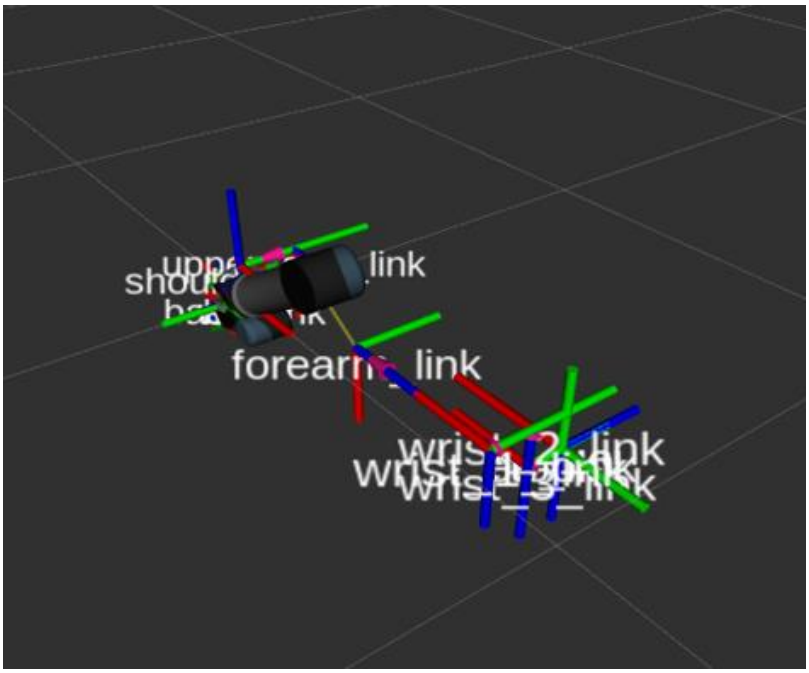

Figure 14:TF

3.3 Experimentation Setup

3.3.1 Setting waypoints

10 waypoints were chosen for calibration such that they spanned toward the extreme points of the camera's view. They are shown below

Figure 15: Waypoints

The waypoints are constant and do not change for any algorithm/pattern used. This is used to ensure that every calibration carried out has constant features and thus, can only be compared using the variables.

3.3.2 Position of Camera

Two fixed positions of the camera were taken into consideration.

a) 100cm from the base of the robot

b) 150cm from the base of the robot

The minimum distance for the camera to produce a good and stable point cloud was calculated to be 1m, thus these distances were taken accordingly.

The camera was placed on a tripod with an angle of 30 deg.

Figure 16:Camera Setup

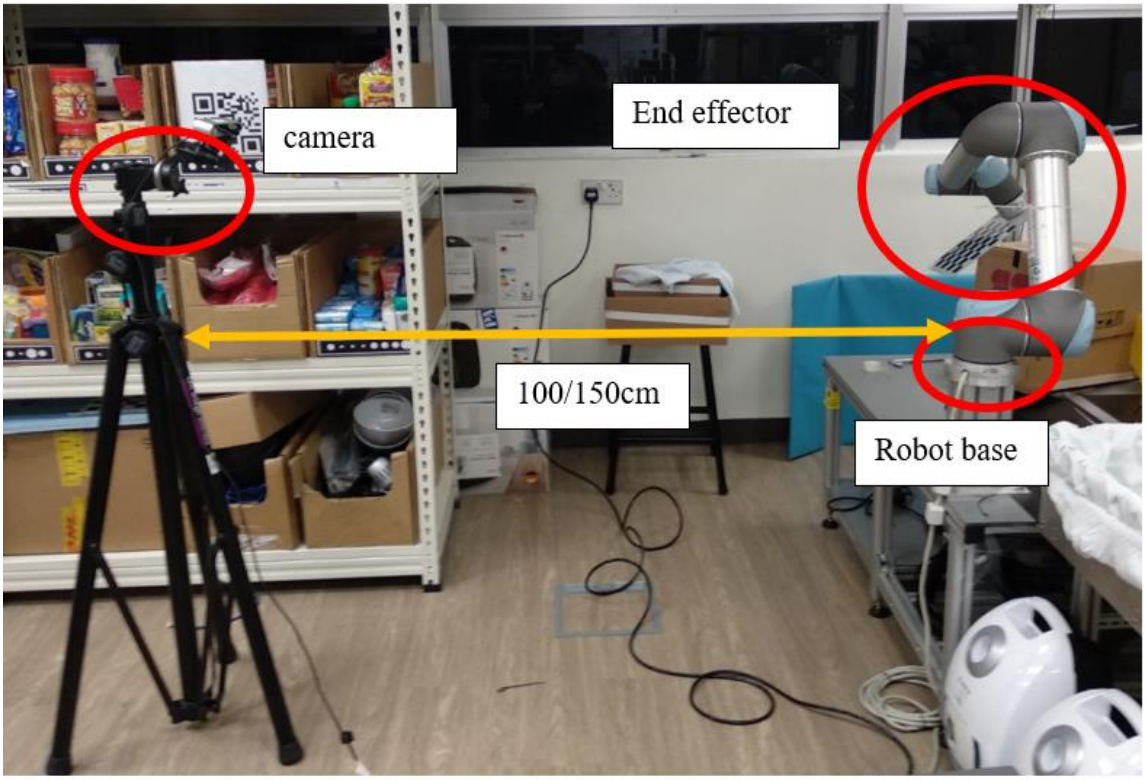

Figure 17: Experimental setup

3.3.3 Markers Used

There were 3 markers that were used namely the checkerboard, Aruco and the Ellipse. These markers were chosen because they are the most common and widely used markers for calibration in the computer vision industry mainly for:

a) ease of detection in different conditions

b) inbuilt libraries in OpenCV for detection of these markers.

I) Checkerboard

The checkerboard provides robust and easy implementation when used in calibration. Even if a part of the calibration pattern is occluded, we can still get the coordinates of the intersection points which is later computed to calculate and identify the chessboard in an image. The lines can be interpolated from sample points helping us get precision and accuracy in detection of these chessboards. An image of the chessboard used in the experimentation along with the specifications is listed below.

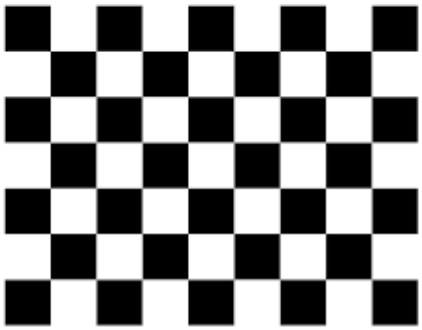

Figure 18:Checkerboard

Specifications:

i. 7x6 (width x height)

ii. size of square: 2.5cm

b) Aruco Marker

Aruco markers are square fiducials that is used for pose estimation and detection. It usually consists of a black border with an internal matrix of binary digits and an identifier. The black box helps to identify the marker with high speed and precision. The marker can be identified in any rotation but requires the original rotation to be determined. Aruco markers are defined by a dictionary. In our experimentation, we have used the Aruco marker defined in the Original dictionary. The marker used along with the specifications is listed below.

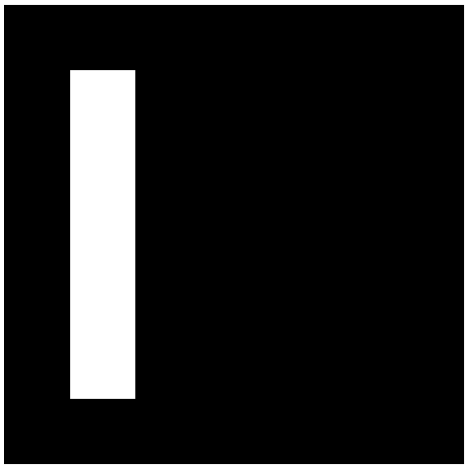

Figure 19:Aruco marker

Specifications:

i. size of each edge – 7cm

c) Ellipse marker

The Ellipse marker is relatively new to the computer vision community. It consists of concentric circles along with black diagonal squares that determine the orientation of the

Ellipse marker. A line passing diagonally through these square tiles is considered to be the Y-coordinate and the line perpendicular to this line is considered to be the X-coordinate. These markers are easily identified using the Hough line transform to identify ellipses and do not require any special formulae to be detected. The Ellipse marker used in our experimentation is shown below along with the specifications.

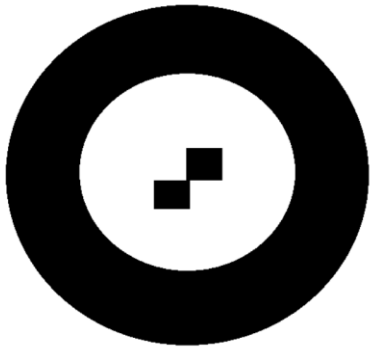

Figure 20:Ellipse marker

Specifications:

i. Outer circle diameter: 9.5cm

ii. Inner circle diameter: 6cm

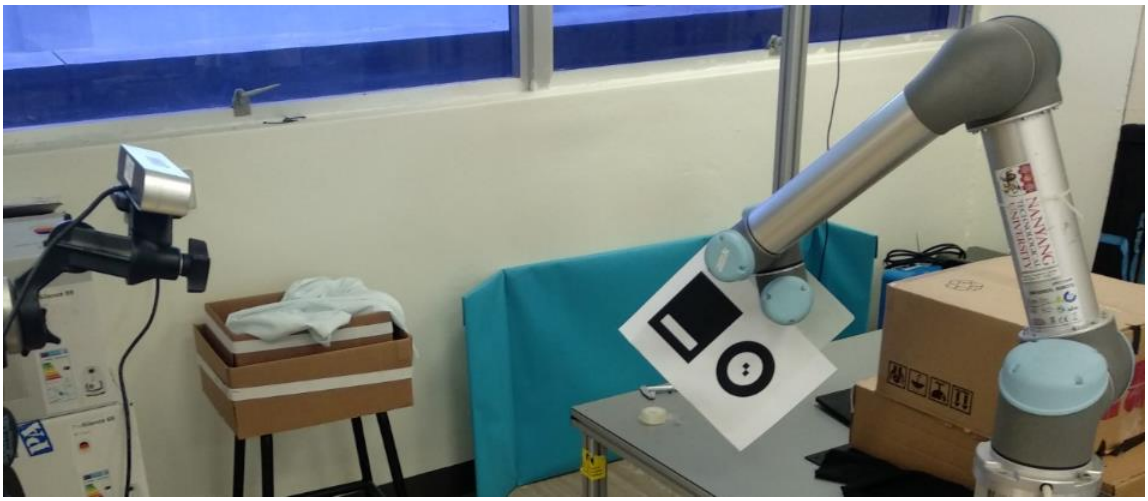

Figure 21: Experimental setup using other markers

Chapter 4: Methodology

This chapter introduces and explains the methodology and the procedure for the experimentation. After the experimental setup was complete, there were several steps that needed to be followed so that the final data could be acquired. These steps are shown as a flowchart below and are explained in further detail in this chapter.

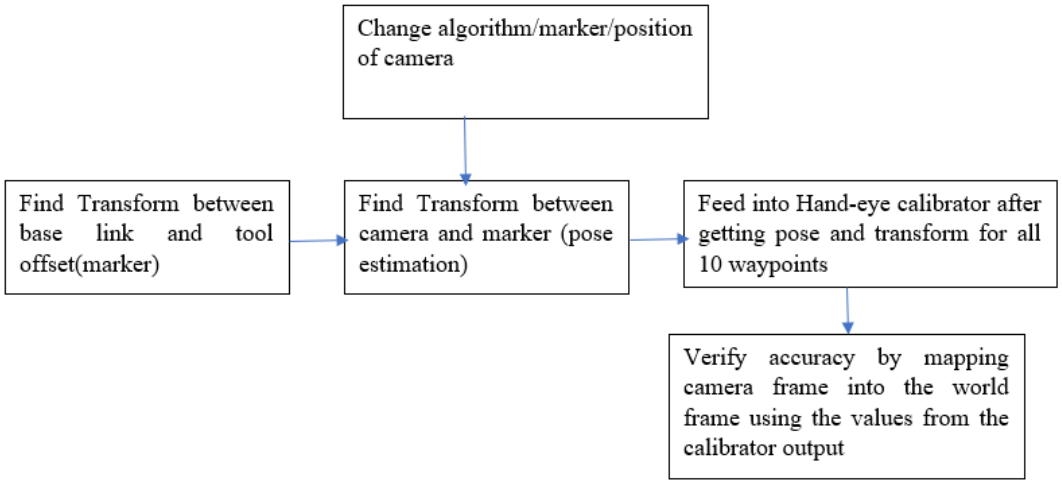

Figure 22:Workflow for Experimentation

4.1 Getting the transformation from robot base to end effector

The transformation from the base link of the robot and end effector is calculated using the Transform broadcaster [17] code present in ROS. After this, the offset from the end effector is added to the end effector to get the point at which the pose of the camera is calculated.

For the checkerboard, the pose is calculated at the right bottom square, therefore the offset is added so that the end effector is transferred to the exact point.

For the Aruco and ellipse markers, the pose is calculated at the centre of the markers, therefore the end effector is offset to the exact point.

These offsets are kept constant throughout and are assumed to be the true values so that the comparison between different configurations gives accurate results.

```
transformation.setOrigin( tf::Vector3(0.190,-0.075, 0) ); //for checkerboard
transformation.setOrigin( tf::Vector3(0.130,0.07, 0) ); //for aruco
transformation.setOrigin( tf::Vector3(0.130,-0.06, 0) ); // for ellipse
```

Figure 23: Code snippet for offsetting pose points

4.2 Parameters Extraction using 2D camera

For checkerboard: All the corners of the checkerboard are detected and stored as the image points. These are fed to the PnP algorithm along with a set of object points keeping the Z as 0 and the width of the points equal to the size of each square.

For Aruco: Aruco markers have a dictionary. Our Aruco used is present in the original Aruco dictionary, the corners of the detected Aruco are taken as the image points and the object points are initialized as the 4 corners with width as specified by the user.

For Ellipse: The two concentric circles provide us with the same centre and the two squares present in the middle provide the orientation. The circles are taken as the image point and the object points are taken with circumference range given.

4.3 Pose Estimation using solvepnp function

The pose for each type of marker is estimated using the image points, object points and the type of algorithm used. Along with these input parameters we should also provide the intrinsic parameters that we obtained from normal internal calibration.

```
cv2.solvePnP(objectPoints, imagePoints, cameraMatrix, distCoeffs[, rvec[, tvec[, useExtrinsicGuess[, flags]]]])
```

Figure 24:Python function for solvepnp

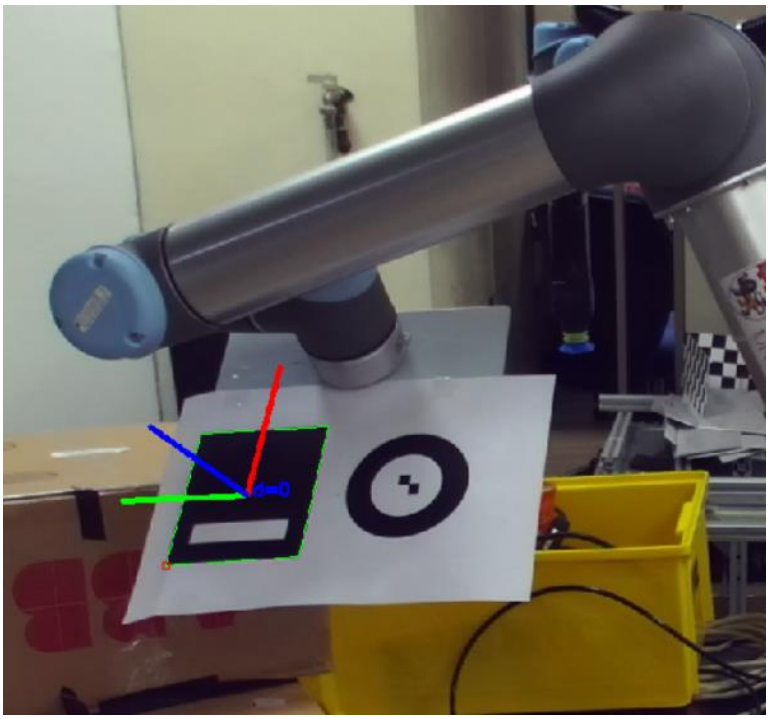

Figure 25:Example Pose estimation for Aruco

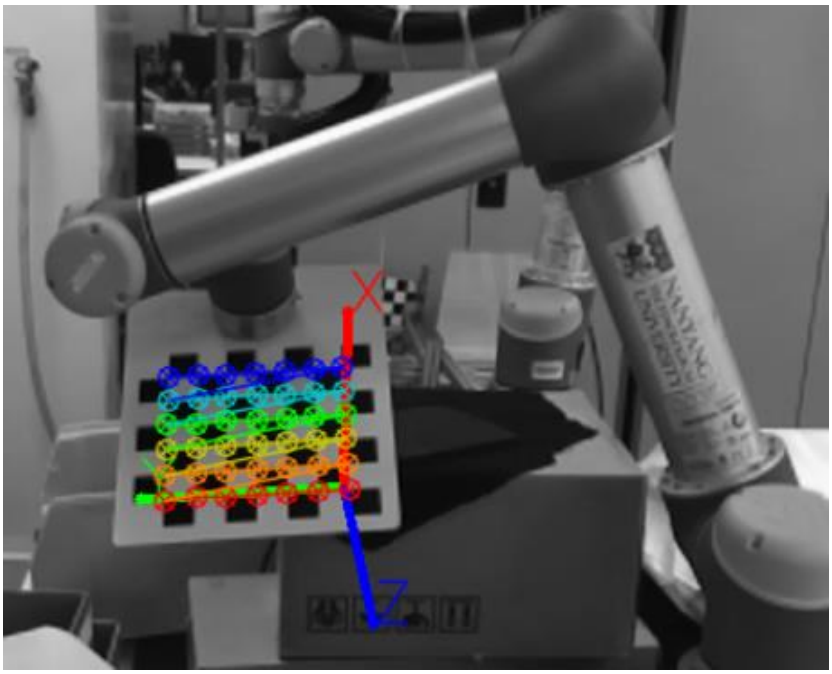

Figure 26:Example pose estimation for checkerboard

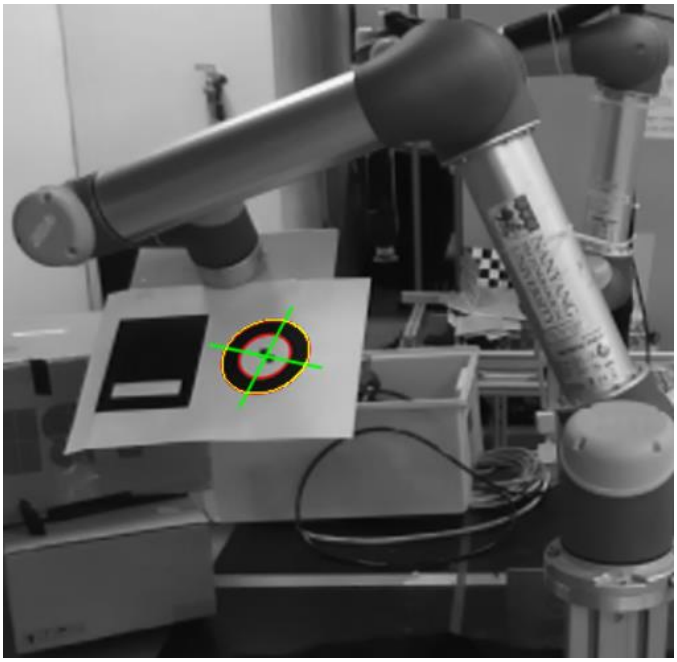

Figure 27: Example pose estimation for ellipse

.

The pose obtained gives us the transformation from the camera to the object and can be mapped in 3d space as a point cloud. The output of a solvepnp function are the rotation and translation vectors which we can use to visualize the pose in 3D.

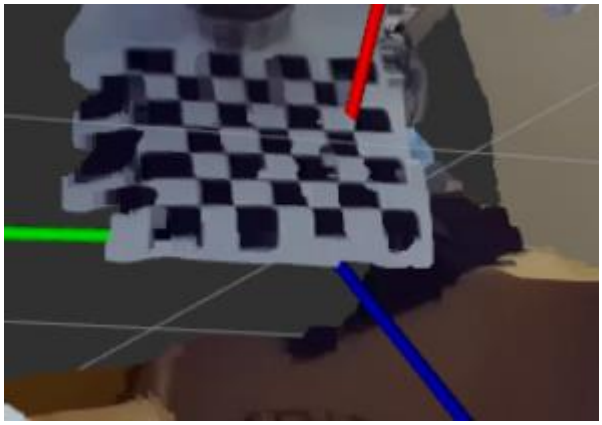

Figure 28: Pose in 3d point cloud

4.4 Errors Encountered with Change in Resolution/Algorithm/Position

Resolution error:

When testing out different resolutions, the VGA (lowest resolution of the camera) was unable to detect checkerboards even at the optimal distance from the robot

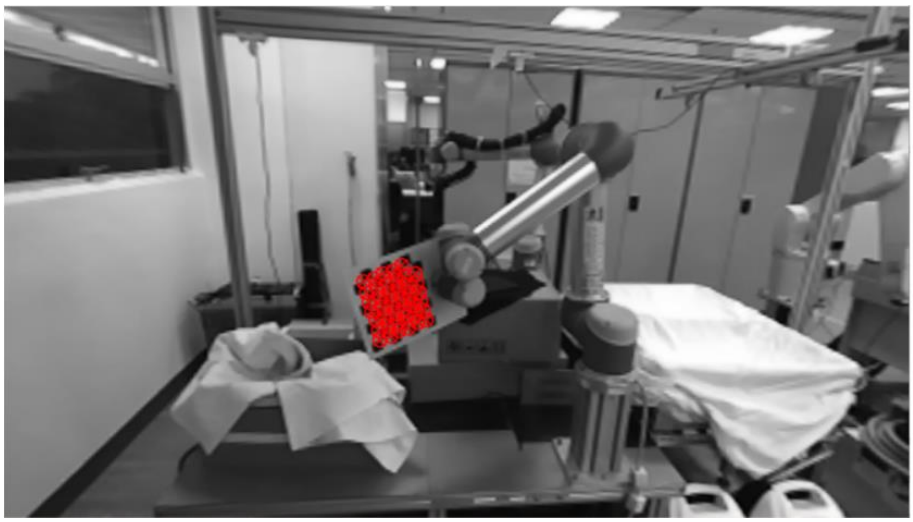

Figure 29:low resolution error

Therefore, this resolution was not taken into consideration while testing out the different algorithms and markers.

Algorithm Implementation error in OpenCV:

When implementing the EPnP and P3P algorithms with OpenCV on checkerboard markers, it was identified that the pose produced in both the 2d and 3d data spaces were wrong, i.e the x and z vectors of the orientation were switched. In the picture below x,y and z refer to red, blue and green. We notice that the red(x) is pointing away from the board which actually signifies the “z” direction.

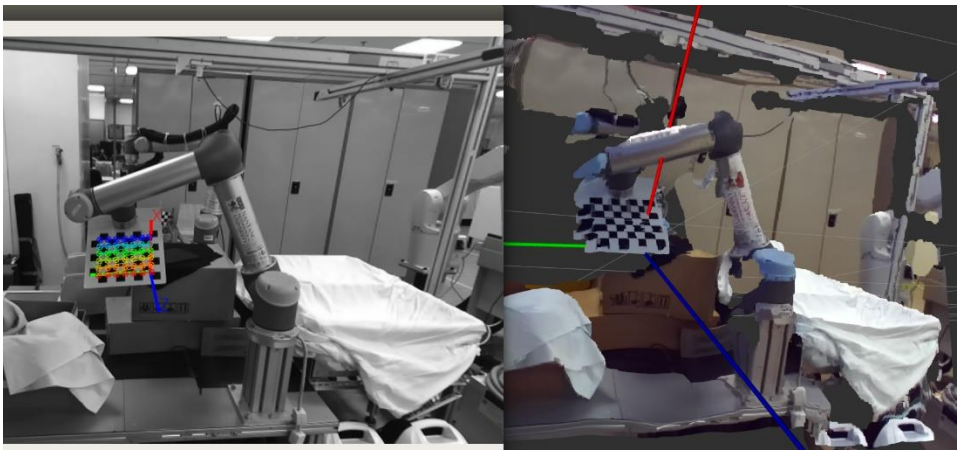

Figure 30:Error in Algorithm

To rectify this, the quaternions were inverted to ensure that the orientation was correct.

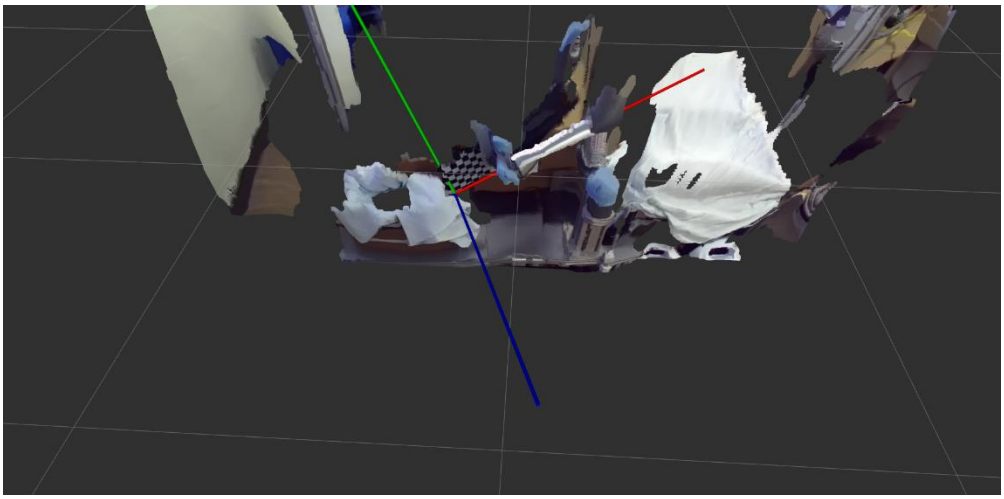

Figure 31:Error rectified

Ellipse errors:

It was noticed that the solvepnp function did not converge for P3P and EPNP when used with the Ellipse marker. Upon further research, the OpenCV implementation was broken for this specific case and thus could not be researched on further.

Distance Errors:

When placed at position 2, the checkerboards were failed to be detected and thus, data could not be collected further. If data was collected for some waypoints, the hand-eye library could not converge to give a stable result for the position of the camera.

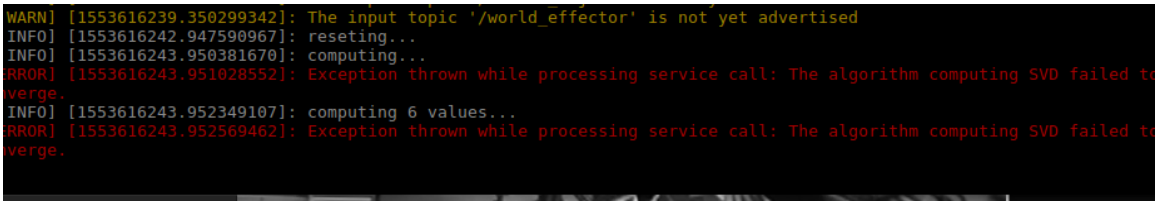

4.5 Hand-eye-calibration

After the pose is identified for all the waypoints, the two transforms are fed into the VISP [18] library to get an output consisting of location and orientation of the camera in the world plane where the robot is situated.

```
Translation: [-0.423, 0.276, 0.076]
Rotation: in Quaternion [-0.383, 0.817, 0.412, 0.126]
         in RPY (radian) [2.400, 0.548, -2.483]
         in RPY (degree) [137.515, 31.411, -142.255]
```

Figure 32: Hand-eye calibration output

4.6 Measuring Accuracy

After hand-eye calibration, the camera frame is mapped to the world frame and the transformations are plotted on the 3D data space. The 3-d distance between the two points are calculated to find out the accuracy.

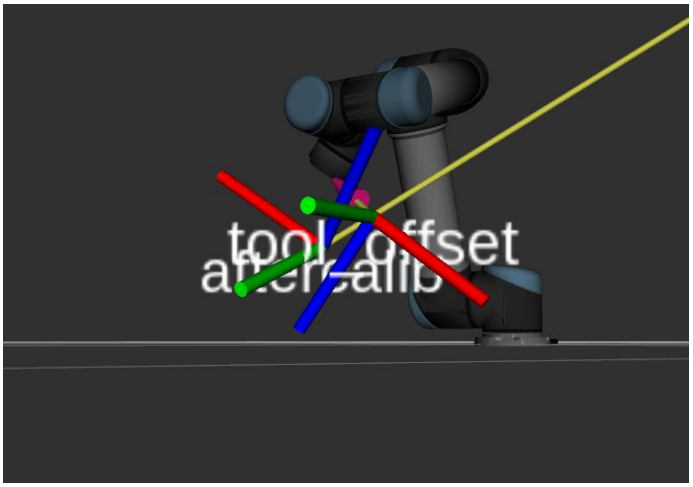

Figure 33:Accuracy measurement

Chapter 5: Results and Discussion

This chapter details all the results obtained after calibration. Once the calibration was carried out for all the 10 waypoints recorded before, the transformation between the camera and the robot base was produced as the output. This transformation represents both the distance and orientation that the camera is present in reference to the base of the robot. Using this transformation, we can map the camera coordinate frame to the robot frame which exists in the world frame. The markers were placed in front of the camera again and identified to represent the pose in the frame of the robot. If the accuracy is hundred percent, there should be no difference between the "tool offset" (Offset from end effector where the marker exists) frame and the "marker pose" (marker pose in relation to the camera) frame. These two poses were recorded and the 3-D Euclidean distance was calculated according to the formula represented below:

We have to ensure that both of these 3-d poses are taken from the same frame id otherwise we will not get accurate results.

Given two points A and B, where A represents the tool offset 3-d point and B represents the marker pose frame

$$A = (x_0, y_0, z_0) \tag{20}$$

$$B = (x_1, y_1, z_1) \tag{21}$$

$$d = \sqrt{(x1 - x0)^2 + (y1 - y0)^2 + (z1 - z0)^2} \quad (22)$$

where

d: distance between two 3-d points

x0, y0, z0: x, y, z coordinates of the first 3d points

x1, y1.z1: x, y, z coordinates of the second 3-d point

All the results have been compared using different criterion and displayed in both tables and graphs so that the information produced can be used when using point correspondence algorithms in the future. The information represents the distance between the tool offset frame (real world coordinates) the marker frame (estimated coordinates). The smaller the distance, the better the accuracy. All the values listed are in meters.

Position 1: 100cm from robot base

Position 2: 150cm from robot base

5.1 Comparison of Algorithms and Markers at Position 1 in 720P resolution

This comparison helps us observe the performance of the various algorithms and markers used at the 720 pixels resolution of the camera used. The values were not able to be estimated for any other algorithms for the Ellipse marker other than the Iterative algorithm as the provisions are not present in OpenCV. These values are listed as “NA”. Even the RANSAC algorithm was used to try and estimate the values for Ellipse in case the error

was being produced by any outliers present in the algorithm inputs but the algorithms were not able to converge and produce the pose required for calibration. The table and graph below represent the data points and visualization of the distances at this configuration.

Table 1: Position 1/720p

Distance between world coordinates and estimated coordinates from calibration			
Algorithms	Markers Used		
	Aruco	Checkerboard	Ellipse
ITERATIVE	0.0954	0.0333	0.178
EPNP	0.0818	0.0364	NA
P3P	0.0868	0.0449	NA

	Checkerboard	Aruco	Ellipse
ITER	0.0326	0.0954	0.179
EPNP	0.0323	0.0818	0
P3P	0.0289	0.0868	0

Figure 34:Position1/720p values

We notice that the accuracy is the highest while using the Checkerboard for all algorithms used as the distance between the real and estimated coordinates have the least value, producing the highest accuracy. While comparing the different algorithms we see that P3P performs the best while using a checkerboard and EPnP while using an Aruco board, but when comparing in general, the accuracy is far greater while using a checkerboard.

5.2 Comparison of Algorithms and Markers at Position 1 in 1080P resolution

This comparison helps us observe the performance of the various algorithms and markers used at the 1080 pixels resolution of the camera used. The values were not able to be estimated for any other algorithms for the Ellipse marker other than the Iterative algorithm for the same reasons as listed in the previous comparison. These values are listed as "NA". The table and graph below represent the data points and visualization of the distances at this configuration. The units of data are in meters and the lesser the value, the greater is the accuracy.

Table 2:Position 1/1080p

Distance between world coordinates and estimated coordinates from calibration			
Algorithms	Markers Used		
	Aruco	Checkerboard	Ellipse
ITERATIVE	0.0912	0.0331	0.179
EPNP	0.164	0.0235	NA
P3P	0.0964	0.0399	NA

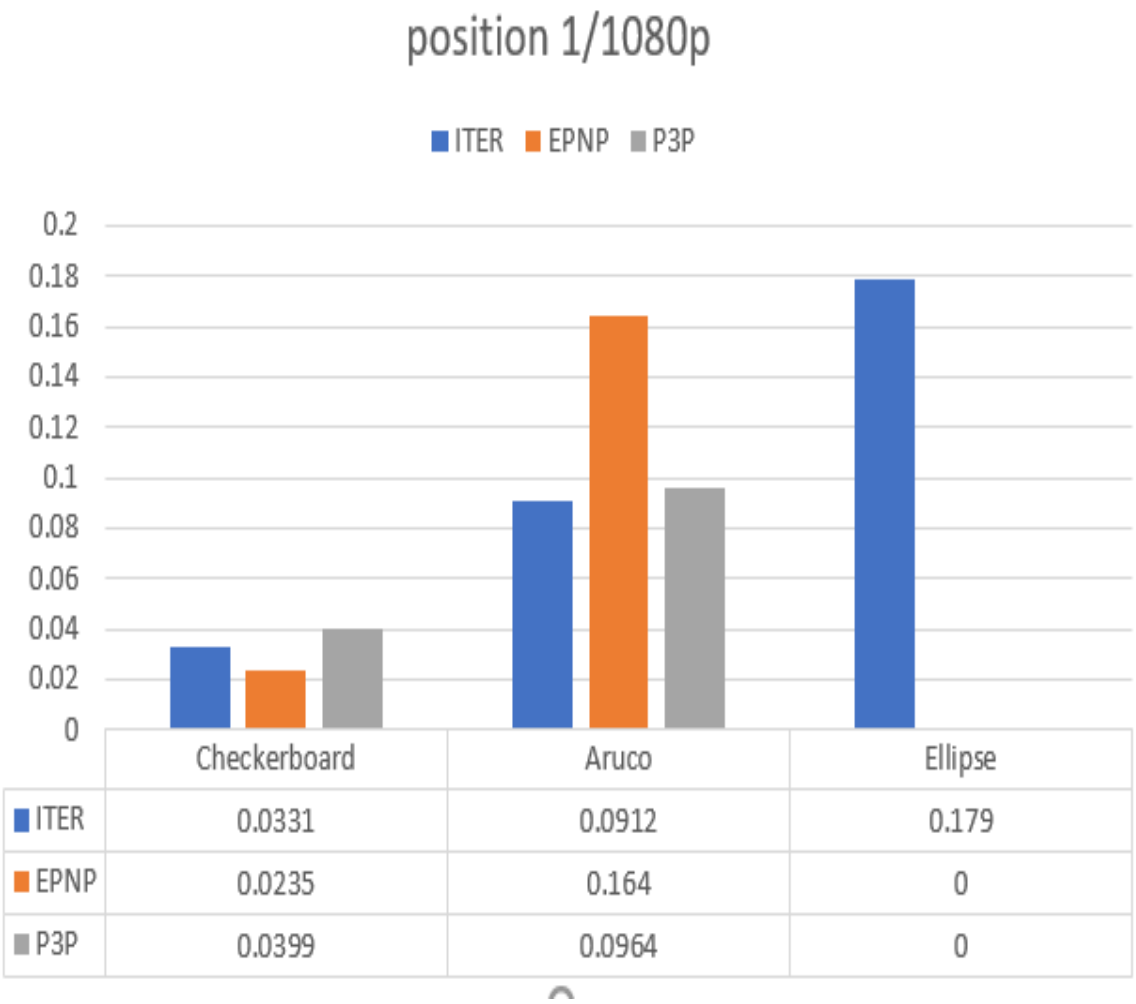

	Checkerboard	Aruco	Ellipse
ITER	0.0331	0.0912	0.179
EPNP	0.0235	0.164	0
P3P	0.0399	0.0964	0

Figure 35:Position1/1080p values

We can notice that again, the accuracy is far greater while using a checkerboard as compared to other markers in this configuration. When we compare the distances individually for each algorithm, we notice that EPnP gives us the best accuracy while using a checkerboard whereas Iterative gives us the best while using the Aruco. There is

no other output for us to compare Ellipses with but the accuracy produced is way lower when compared with the other two markers.

5.3 Comparison of Algorithms and Markers at Position 1 in 2KHD resolution

This comparison helps us observe the performance of the various algorithms and markers used at the 2KHD (2.2k) pixels resolution of the camera used. The values were not able to be estimated for any other algorithms for the Ellipse marker other than the Iterative algorithm for the same reasons as listed in the previous comparison. These values are listed as "NA". The table and graph below represent the data points and visualization of the distances at this configuration. The units of data are in meters and the lesser the value, the greater is the accuracy.

Table 3: Position 1/2KHD

Distance between world coordinates and estimated coordinates from calibration			
Algorithms	Markers Used		
	Aruco	Checkerboard	Ellipse
ITERATIVE	0.0832	0.0333	0.178
EPNP	0.101	0.0364	NA

P3P	0.101	0.0449	NA

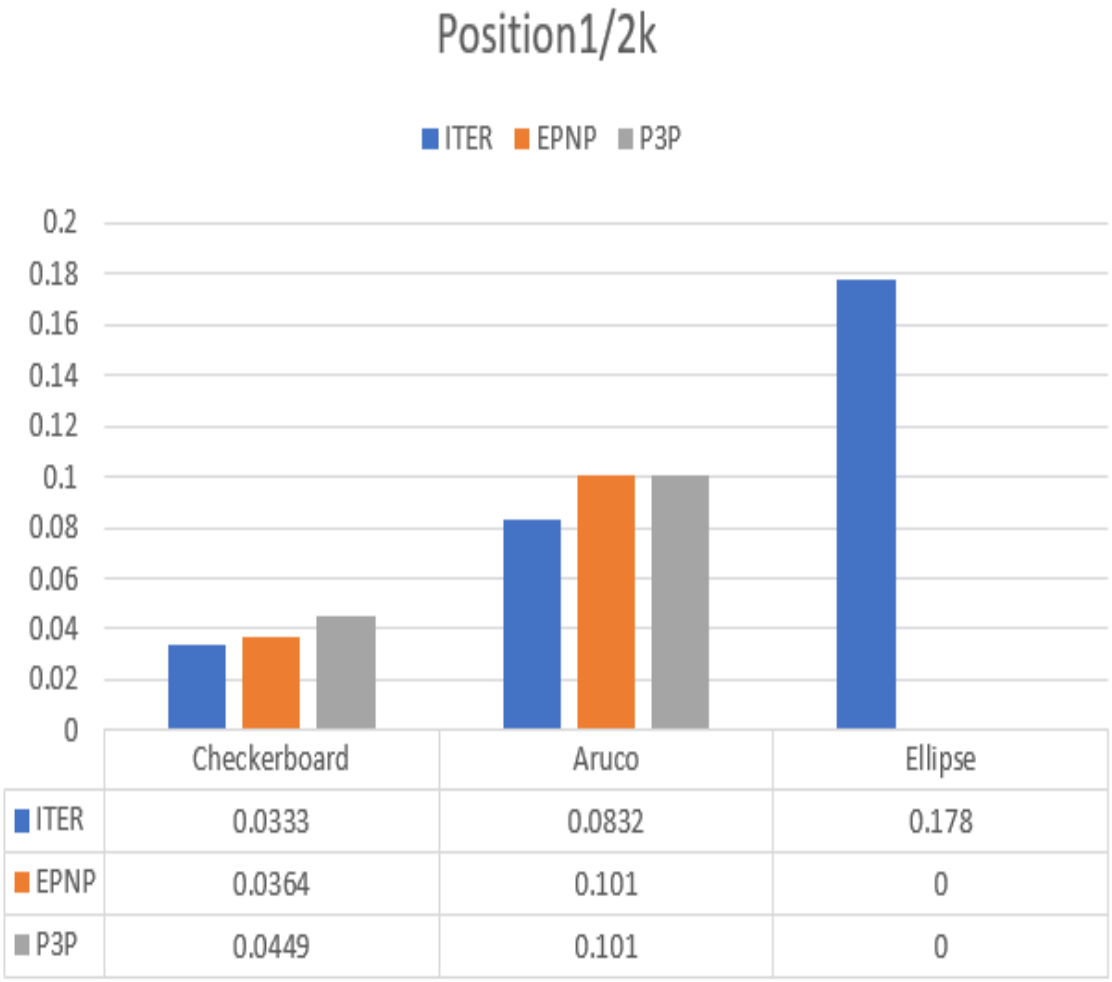

Figure 36:Position 1/2k

While using the maximum resolution of the Zed camera, we notice that the Checkerboard provides the best accuracy again but this time, the iterative algorithm produces the best accuracy while using the checkerboard. Again, we see that the iterative produces the best accuracy while using the Aruco board at the highest resolution. There is no other output

for us to compare Ellipses with but the accuracy produced is way lower when compared with the other two markers.

5.4 Comparison of Algorithms and Markers at Position 2 in 720P resolution

This comparison helps us observe the performance of the various algorithms and markers used at the 720 pixels resolution of the camera used. The values were not able to be estimated for any other algorithms for the Ellipse marker other than the Iterative algorithm for the same reasons as listed in the previous comparison. The checkerboard was not able to be identified from this position as shown in figure 28 as the sizes of the squares in the checkerboard are too small for the algorithm to detect the board. These unidentified values are listed as “NA”. The resolution was not compared at this position due to poor detection of the markers and unavailability of a solution for incorporating the Ellipse marker for algorithms other than the Iterative algorithm. The table and graph below represent the data points and visualization of the distances at this configuration.

Table 4:Position 2/720P

Distance between world coordinates and estimated coordinates from calibration			
Algorithms	Markers Used		
	Aruco	Checkerboard	Ellipse
ITERATIVE	0.224	NA	0.178
EPNP	0.143	NA	NA
P3P	0.149	NA	NA

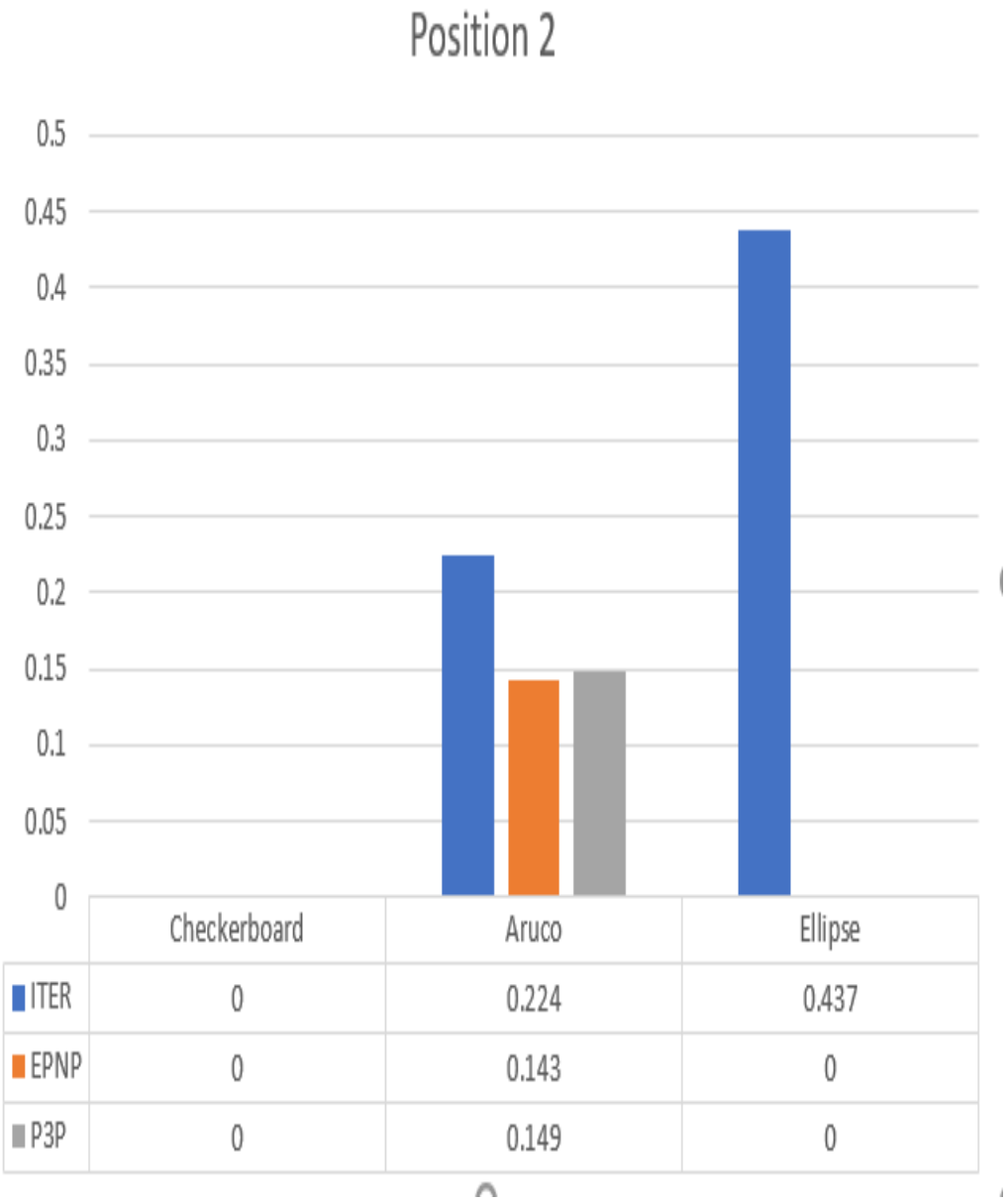

Figure 37:Position2

As we can see from the graph, the only stable results produced are from the Aruco marker. The checkerboard was not able to be identified and the algorithms were not able to converge for the Ellipse pose to be detected. The checkerboard non-identification problem

could be solved by increasing the size of the checkerboard size but since we had set it as a control variable, changing it would alter the results. The Aruco marker produces the best accuracy with the EPnP algorithm. Again, we notice that the Ellipse accuracy is far lower than Aruco.

5.5 Comparison of Algorithms for Checkerboard Marker at all resolutions (Position 1)

As position 2 did not provide us with suitable results, the algorithms were compared for various resolutions at Position 1 for different algorithms used. The units of data are in meters and the lesser the value signifies greater accuracy. The table and graph displayed below help visualize how each algorithm fares in each case.

Table 5:Checkerboard comparison

Distance between world coordinates and estimated coordinates from calibration (Checkerboard)			
Algorithms	Resolution		
	720P	1080P	2KHD
ITERATIVE	0.0326	0.0331	0.0333
EPNP	0.0323	0.0235	0.0364

P3P	0.0289	0.0399	0.0449

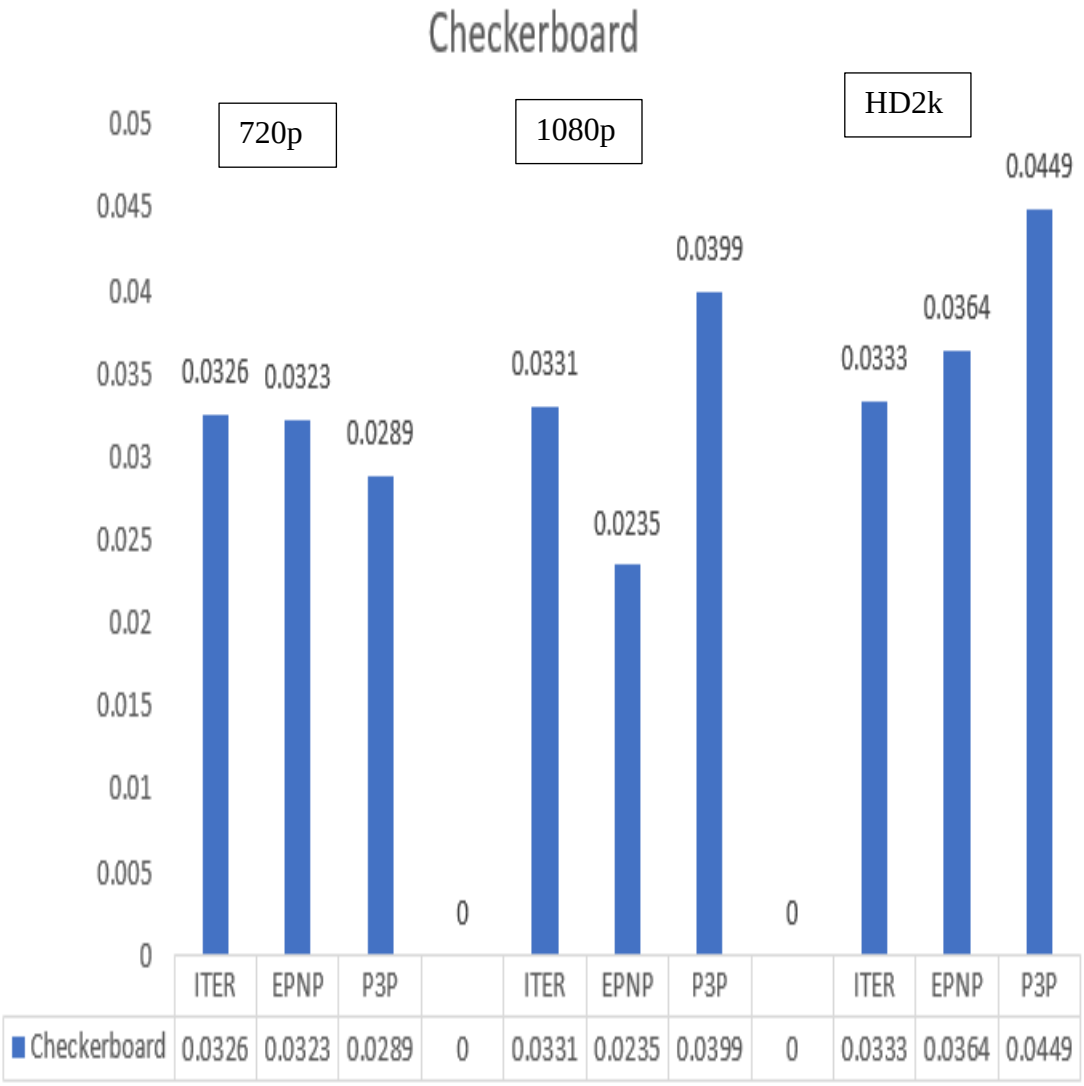

Figure 38:Comparing Checkerboard

We notice that the highest accuracy is achieved when the resolution is at 1080p using the EPnP algorithm. When comparing the algorithms at the 720P configuration, we notice that the P3P algorithm produces the best accuracy and the Iterative algorithm when

compared at the 2KHD configuration. For the Iterative and P3P algorithm, the best accuracy is achieved at 720p. We also can notice a general decrease in accuracy as the resolution increases.

5.6 Comparison of Algorithms for Aruco Marker at all resolutions (Position 1)

Even though position 2 did provide us with suitable results, the algorithms were compared for various resolutions at Position 1 for different algorithms used to provide a basis for comparison with the other markers. The units of data are in meters and the lesser the value signifies greater accuracy. The table and graph displayed below help visualize how each algorithm fares in each case.

Table 6: Aruco comparison

Distance between world coordinates and estimated coordinates from calibration (Aruco)			
Algorithms	Resolution		
	720P	1080P	2KHD
ITERATIVE	0.0954	0.0912	0.0832
EPNP	0.0818	0.164	0.101

P3P	0.0868	0.0964	0.101

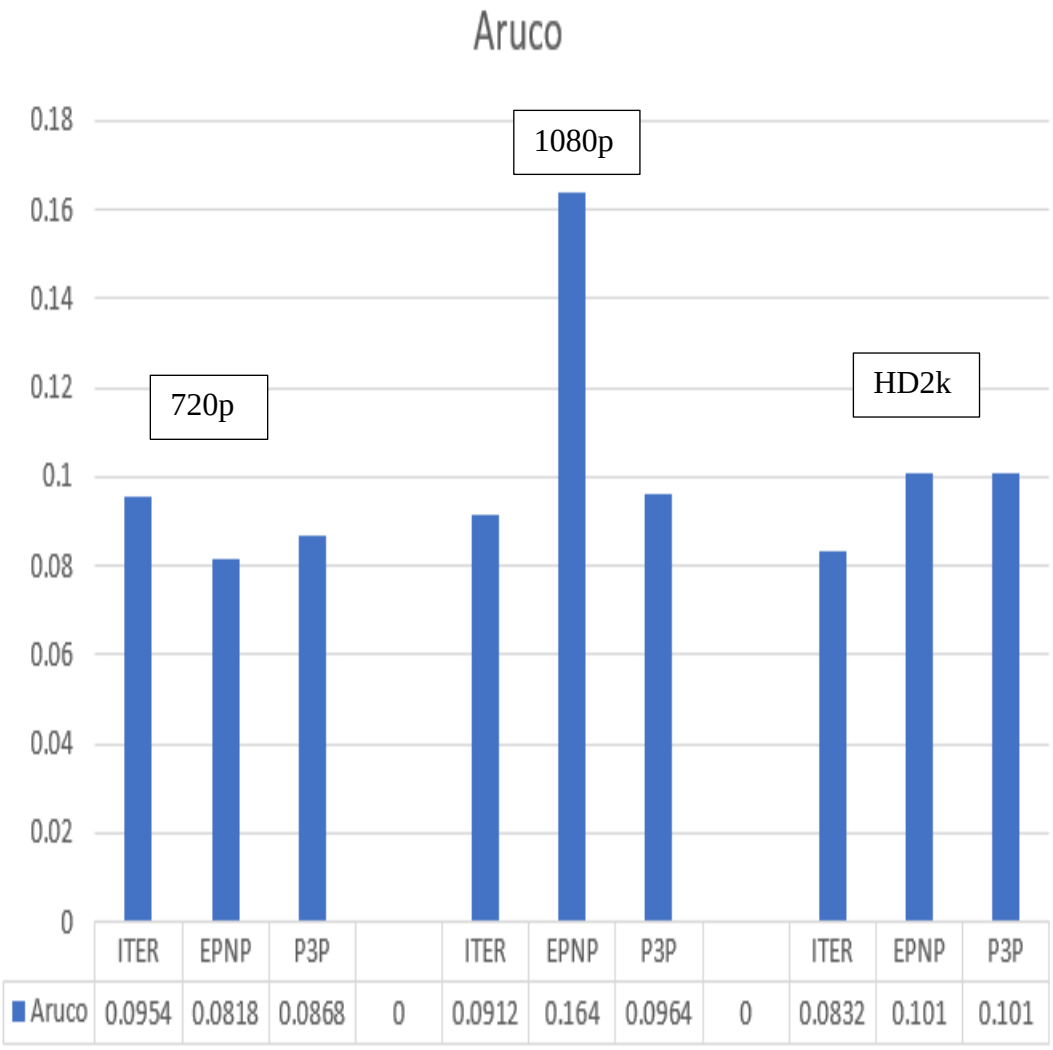

Figure 39:Comparing Aruco

When using the Aruco marker, we can notice that the best accuracy is achieved at 720p using the EPnP algorithm. If the 1080p or HD2k resolution is used, the Iterative algorithm produces the best accuracy. We also see a similar trend where accuracy reduces as the resolution increases when using the EPnP and P3P algorithm

5.6 Comparison of Algorithms for the Ellipse Marker at all resolutions (Position 1)

The Ellipse marker only worked with the Iterative algorithm at any position and resolution. This led to a very small dataset that allowed us to compare with other markers. Using the possible information that was able to be obtained, a comparison was plotted for various resolutions at Position 1. This position was chosen to be visualized as it provided us with a basis for comparisons with other markers (checkerboard fails at position 2). The units of data are in meters and the lesser the value signifies greater accuracy. The table and graph displayed below help visualize how each algorithm fares in each case.

Table 7: Ellipse comparison

Distance between world coordinates and estimated coordinates from calibration (Ellipse)			
Algorithms	Resolution		
	720P	1080P	2KHD
ITERATIVE	0.179	0.179	0.178
EPNP	NA	NA	NA

P3P	NA	NA	NA

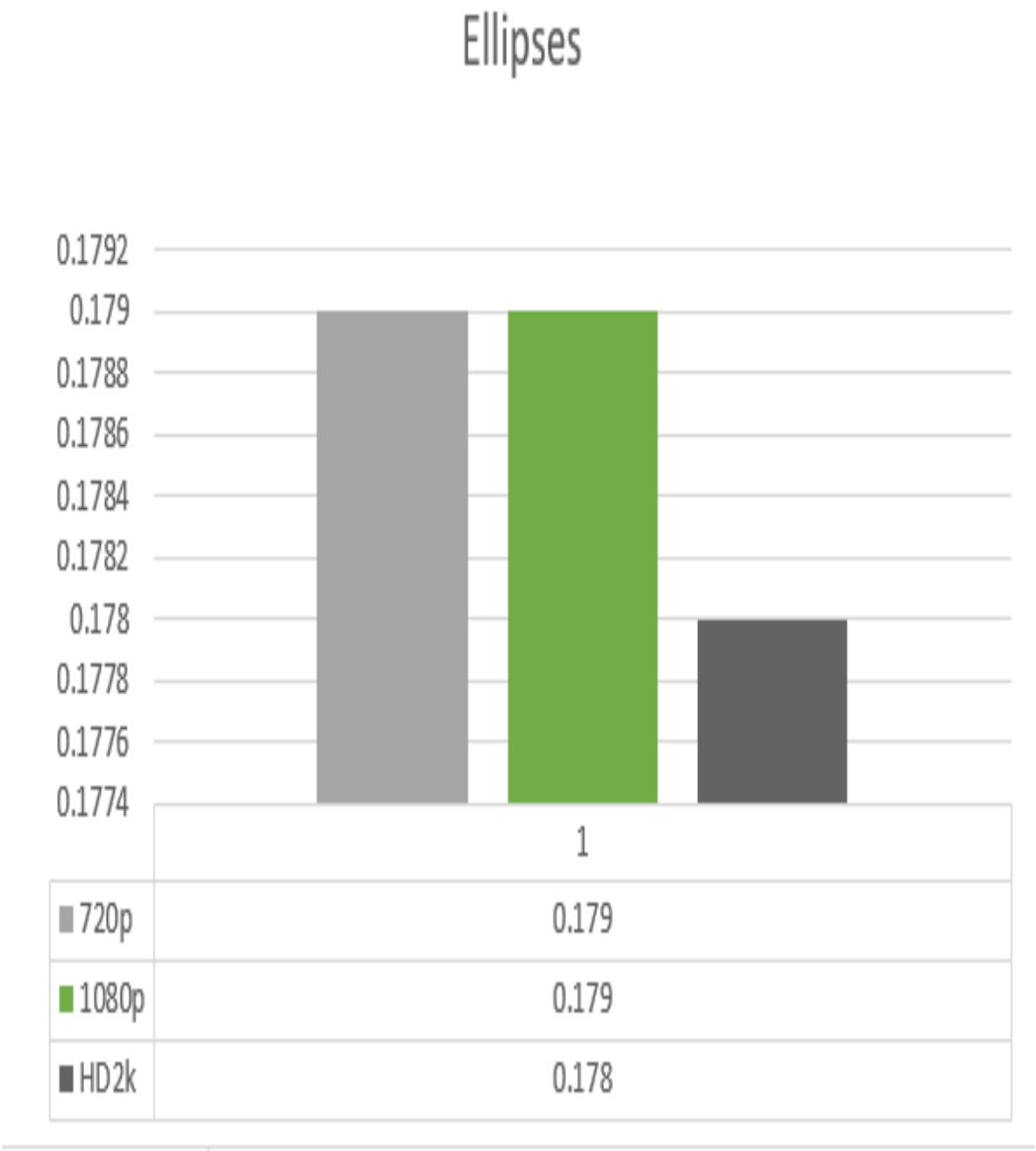

Figure 40:Comparing Ellipses

We notice that the Ellipse does not converge for other algorithms other than the Iterative algorithm. For all the three resolutions, the distance between the real and estimated coordinates have very similar values. These values, upon further inspection seem to be of a greater value (17.8cm – 17.9cm) as compared to other values (< 10cm). The Ellipse thus produces accuracies of a lower degree when compared to the other markers.

5.7 Comparison of Algorithms for different positions

The checkerboard was failed to be detected in position 2 and produced no poses for calibration. Similarly, the pose was not able to be calculated for the Ellipse marker for any other algorithm other than Iterative. The only marker that was detected and produced stable results was the Aruco marker. Thus, this marker was selected to compare the accuracies at different positions of the camera with respect to the robot base. The units of data are in meters and the lesser the value signifies greater accuracy. The table and graph displayed below help visualize how each algorithm fares in each case.

Table 8: Position comparison at 720P using Aruco

Distance between world coordinates and estimated coordinates from calibration for different positions at 720P (Aruco)

Algorithms	Position of camera	
	Position 1 = 100cm	Position 2 = 150cm
ITERATIVE	0.0954	0.224
EPNP	0.0818	0.143
P3P	0.0868	0.149

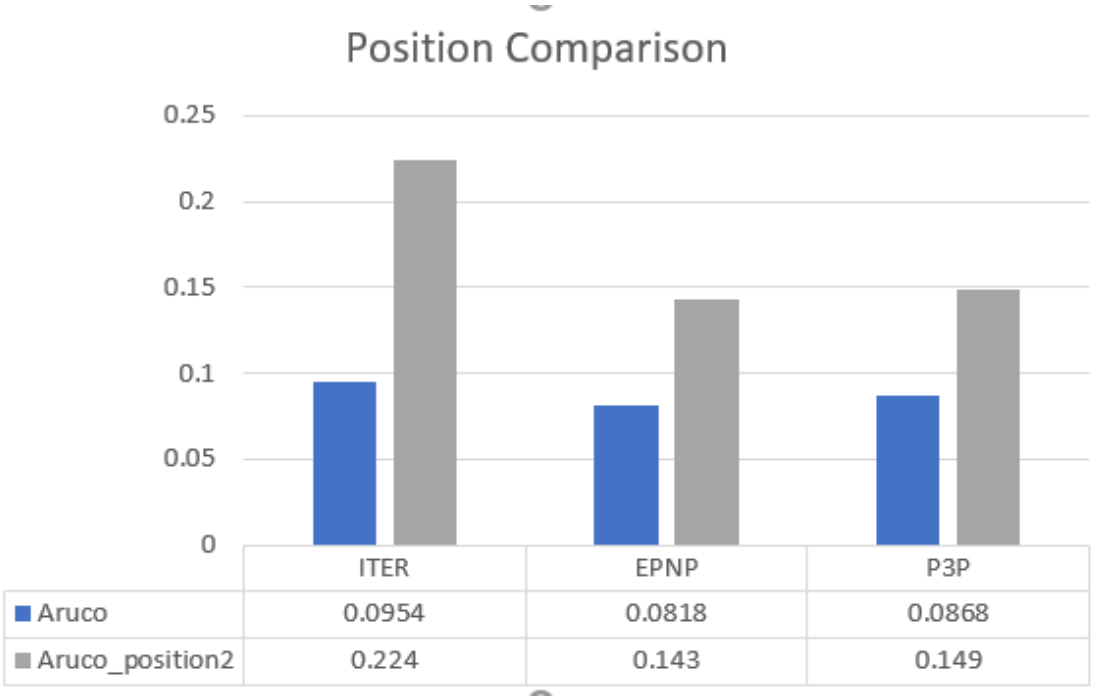

Figure 41:Position comparison at 720P using Aruco

We can notice that the distance increases in position 2 for each algorithm signifying a reduction in accuracy as we move away from the base of the robot. The EPnP algorithm produces the best results for both the positions. This might be due to the fact that it is tested under 720p resolution and as shown in the previous comparisons, the EPnP algorithm works the best under this resolution for the Aruco marker.

Chapter 6- Summary and Future work

6.1 Summary

In this dissertation, different Point correspondence methods were compared by testing them under various conditions and with different markers. It was noticed that for certain conditions, certain algorithms and markers worked well. The checkerboard marker works the best when the distance is comparable(50-120cm) from the robot. If the distance increases, we notice that the camera is not able to identify the checkerboard squares. The ellipses produce the least accuracy while calibrating. This might be due to the fact that the orientation of the ellipse was misaligned to the board. Therefore, it is essential that the orientation of the Ellipse marker always aligns with the board without any deviation. This might produce better results if tested in the future. Also the Ellipses were not able to work with other algorithms such as P3P and EPnP and therefore need to be fixed in the OpenCV library. The Aruco marker was able to be detected at both the locations and produced considerable accuracy at both. For easy and fast implementation, Aruco marker can be prescribed while using the respective algorithm at the desired resolution. The resolution played a role in accuracy. With increase in resolution we could notice a decrease in accuracy of the calibration. This might be due to the fact that the algorithm had to search through more points when detecting the markers. The position of the camera has an inverse relation with the accuracy of calibration. As we moved the camera away, we could see a decrease in accuracy of both Aruco and Ellipse marker setups. There was no clear winner

while using the algorithms as each algorithm produced good results under different conditions. It was henceforth proved that we need not only rely on the Iterative algorithm that the solvepnp function uses by default and we can use the information given above to choose our algorithm and marker according to the needs of our objective.

6.2: Future Work

Once the P3P and EPnP functions are fixed in the OpenCV library we can test these algorithms with the Ellipse markers thus allowing us to have more choices while selecting an algorithm. More conditions can be taken into account while trying to setup experiments such as illumination, noise in images and eye-in hand configurations while performing calibration. This thesis has considered only algorithms that are common and widely used. Other algorithms such as UPnP can be also tested and compared for a greater choice. Along with testing the accuracy, the speed of calibration and detection can also be tested. Other markers can also be used such as QR codes. This will help develop a dataset that the community can use while using point correspondence algorithms.

Bibliography

1. V. Popescu, B. Benes, P. Rosen, J. Cui and L. Wang, "A Flexible Pinhole Camera Model for Coherent Nonuniform Sampling" in IEEE Computer Graphics and Applications, vol. 34, no. 04, pp. 30-41, 2014.

2. E. Marchand, "VISP: a software environment for eye-in-hand visual servoing," Proceedings 1999 IEEE International Conference on Robotics and Automation (Cat. No.99CH36288C), Detroit, MI, USA, 1999, pp. 3224-3229 vol.4.
doi: 10.1109/ROBOT.1999.774089

3. "Camera Calibration and 3D Reconstruction¶." *Camera Calibration and 3D ReconstructionOpenCV2.4.13.7Documentation*,docs.opencv.org/2.4/modules/calib3d/doc/camera_calibration_and_3d_reconstruction.html?highlight=solvepnp.

4. M. H. Merzban, M. Abdellatif and A. A. Abouelsoud, "A simple solution for the non perspective three point pose problem," *2014 International Conference on 3D Imaging (IC3D)*,Liege,2014,pp1-6.

5. T. Shao-xiong, L. Shan and L. Zong-ming, "Levenberg-Marquardt algorithm based nonlinear optimization of camera calibration for relative measurement," *2015 34th Chinese Control Conference (CCC)*,Hangzhou,2015,pp.4868-4872.
doi: 10.1109/ChiCC.2015.7260394

6. S. Basterrech, S. Mohammed, G. Rubino and M. Soliman, "Levenberg—Marquardt Training Algorithms for Random Neural Networks," in *The Computer Journal*, vol. 54, no.1,pp.125-135,Jan.2011.
doi: 10.1093/comjnl/bxp101

7. D. O. Anggriawan, A. Luki Satriawan, I. Sudiharto, E. Wahjono, E. Prasetyono and A. Tjahjono, "Levenberg Marquardt Backpropagation Neural Network for Harmonic Detection," *2018 International Electronics Symposium on Engineering Technology and Applications (IES-ETA)*, Bali, 2018, pp. 129-132.

8. W. Pannao and C. Pintavirooj, "Application of direct linear transform for calibration of miniature computed tomography," *The 5th 2012 Biomedical Engineering International Conference*,UbonRatchathani,2012,pp1-5.
doi: 10.1109/BMEiCon.2012.6465468

9. A. Shahzad, Y. Mu and X. Gao, "Tracking RGB color markers through DLT calibrated monocular vision system," *2016 IEEE International Conference on Mechatronics and Automation*,Harbin,2016,pp.317-321.
doi: 10.1109/ICMA.2016.7558581

10. K. Bai, Chengyin, Liuqin and Gaoming, "Utilization of DLT Theory in 2D Image Analysis System," *2010 Second World Congress on Software Engineering*, Wuhan, 2010, pp.279-282.
doi: 10.1109/WCSE.2010.108

11. B. Zhang, S. Sun, J. Sun, Z. Chi and C. Xi, "3D Reconstruction Method from Biplanar Radiography Using DLT Algorithm: Application to the Femur," *2010 First International Conference on Pervasive Computing, Signal Processing and Applications*, Harbin, 2010, pp. 251-254.

12. F. Vigueras, A. Hernández and I. Maldonado, "Iterative Linear Solution of the Perspective n-Point Problem Using Unbiased Statistics," *2009 Eighth Mexican International Conference on Artificial Intelligence*,Guanajuato,2009,pp.59-64.
doi: 10.1109/MICAI.2009.39

13. L. Wang, Q. Zhang, Z. Wang and S. Cheng, "Fused pose estimation using geometric and texture information," *2017 Chinese Automation Congress (CAC)*, Jinan, 2017, pp. 4221-4224.
doi: 10.1109/CAC.2017.8243520

14. L. D'Alfonso, E. Garone, P. Muraca and P. Pugliese, "P3P and P2P problems with known camera and object vertical directions," *21st Mediterranean Conference on Control and automation, China*

15. W. Ting, W. Yuecao and Y. Chen, "Some Discussion on the Conditions of the Unique Solution of P3P Problem," *2006 International Conference on Mechatronics and Automation*, Luoyang, Henan, 2006, pp. 205-210.
doi: 10.1109/ICMA.2006.257497

16. Yingming Hao, Feng Zhu, Jinjun Ou, Qingxiao Wu, J. Zhou and Shuangfei Fu, "Robust analysis of P3P pose estimation," *2007 IEEE International Conference on Robotics and Biomimetics (ROBIO)*, Sanya, 2007, pp. 222-226.
doi: 10.1109/ROBIO.2007.4522164

17. J. Funda and R. P. Paul, "A comparison of transforms and quaternions in robotics," *Proceedings. 1988 IEEE International Conference on Robotics and Automation*,Philadelphia,PA,USA,1988,pp.886-891vol.2.
doi: 10.1109/ROBOT.1988.12172

18. E. Marchand, "VISP: a software environment for eye-in-hand visual servoing," *Proceedings 1999 IEEE International Conference on Robotics and Automation (Cat. No.99CH36288C)*, Detroit, MI, USA, 1999, pp. 3224-3229 vol.4. doi: 10.1109/ROBOT.1999.774089